

High resolution precipitation mapping in Iceland by dynamical downscaling of ERA-40 with a linear model of orographic precipitation. Appendix [with corrections]

Philippe Crochet

High resolution precipitation mapping in Iceland by dynamical downscaling of ERA-40 with a linear model of orographic precipitation. Appendix [with corrections]

Philippe Crochet, Icelandic Met Office

Contents

Appendix	7
I Monthly precipitation at raingauge stations	8
II Winter precipitation on Hofsjökull	12
III Winter precipitation on Vatnajökull	20
IV Winter precipitation on Langjökull	26
V Statistical characteristics of daily precipitation (1991–2000)	30
VI Annual precipitation maps (1987–2001)	39
VII Mean monthly precipitation maps (1987–2001)	48

Appendix

I Monthly precipitation at raingauge stations

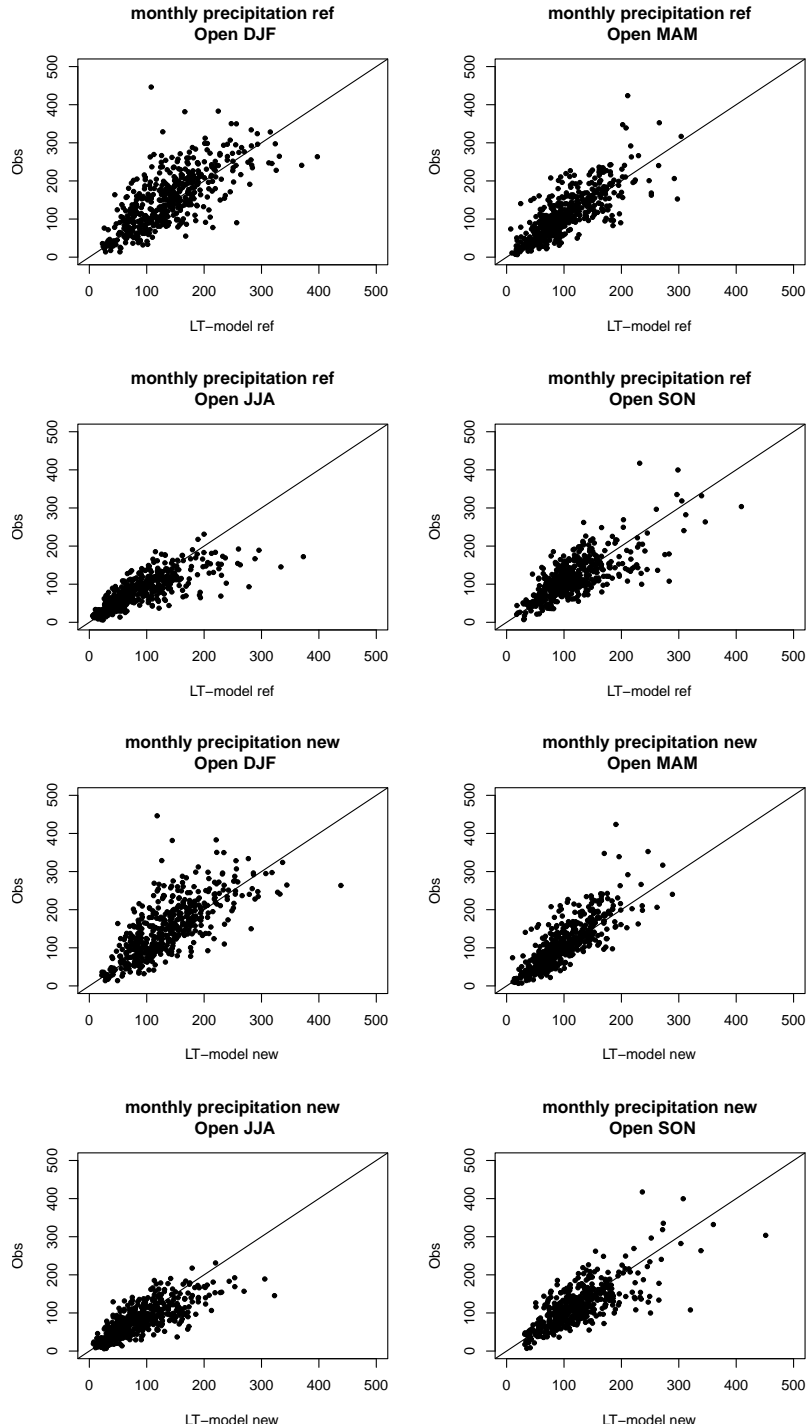


Figure I.1. Monthly precipitation for each season, at stations located in open terrain and simulated with the reference model version (top 4 plots) and the new model version (bottom 4 plots).

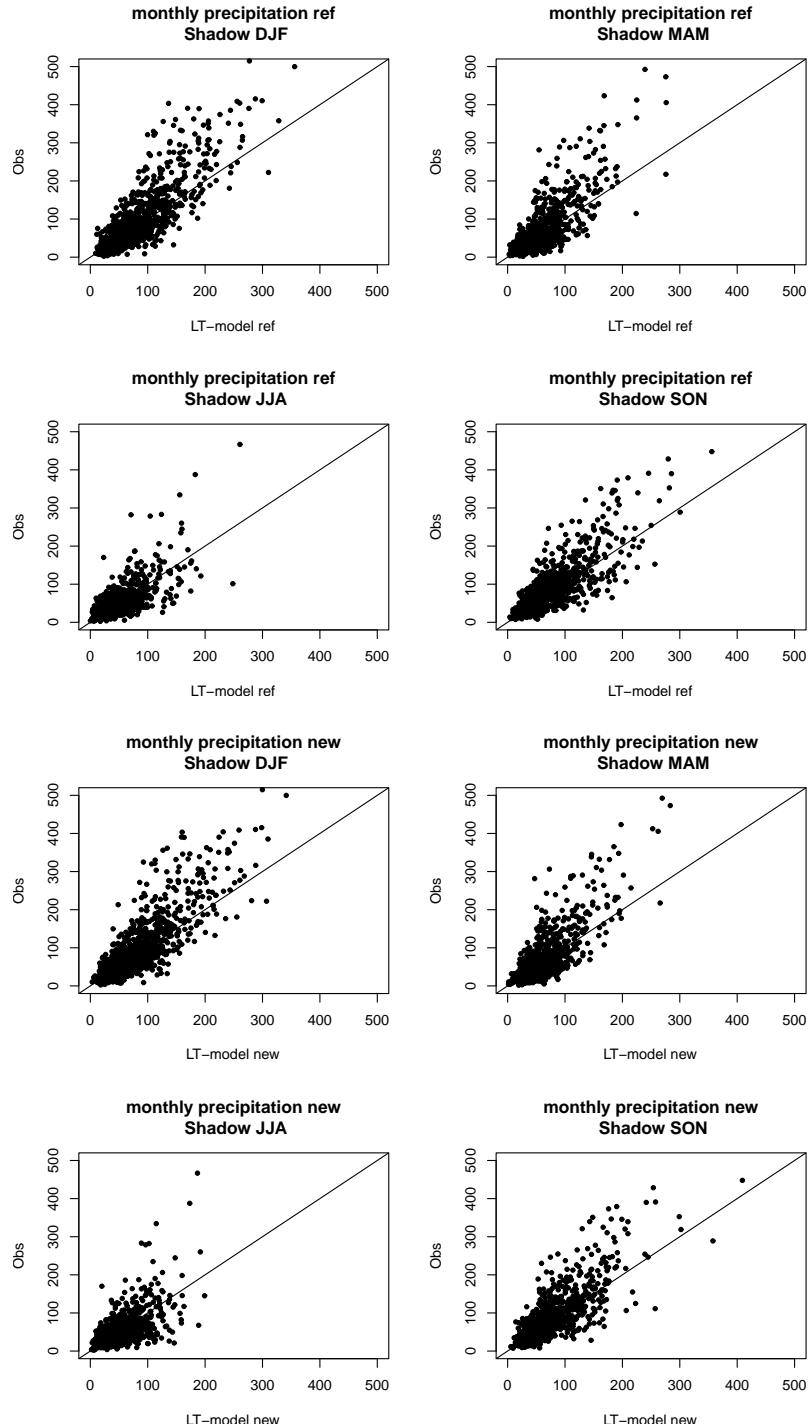


Figure I.2. Monthly precipitation for each season, at stations located in rain-shadow terrain and simulated with the reference model version (top 4 plots) and the new model version (bottom 4 plots).

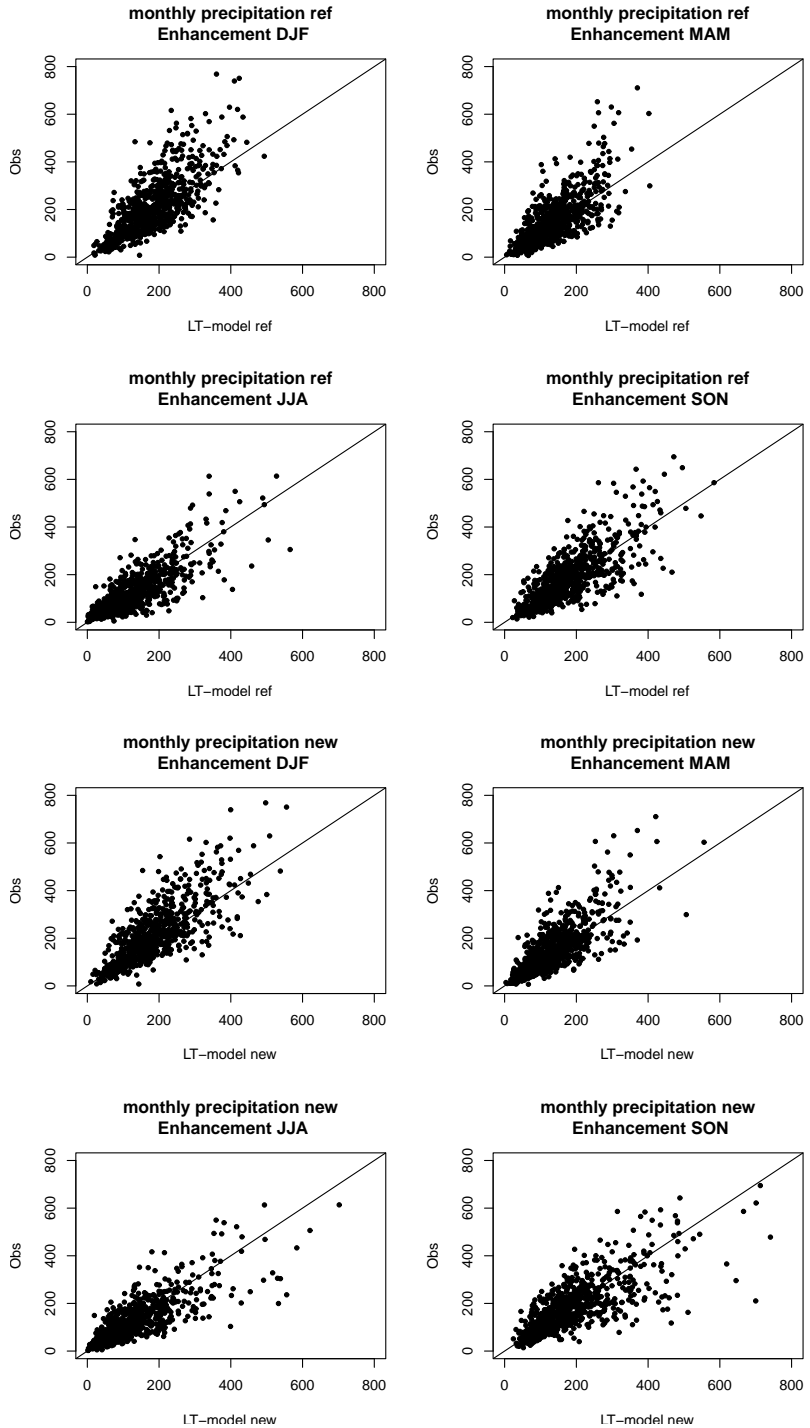


Figure I.3. Monthly precipitation for each season, at stations located in windward terrain and simulated with the reference model version (top 4 plots) and the new model version (bottom 4 plots).

II Winter precipitation on Hofsjökull

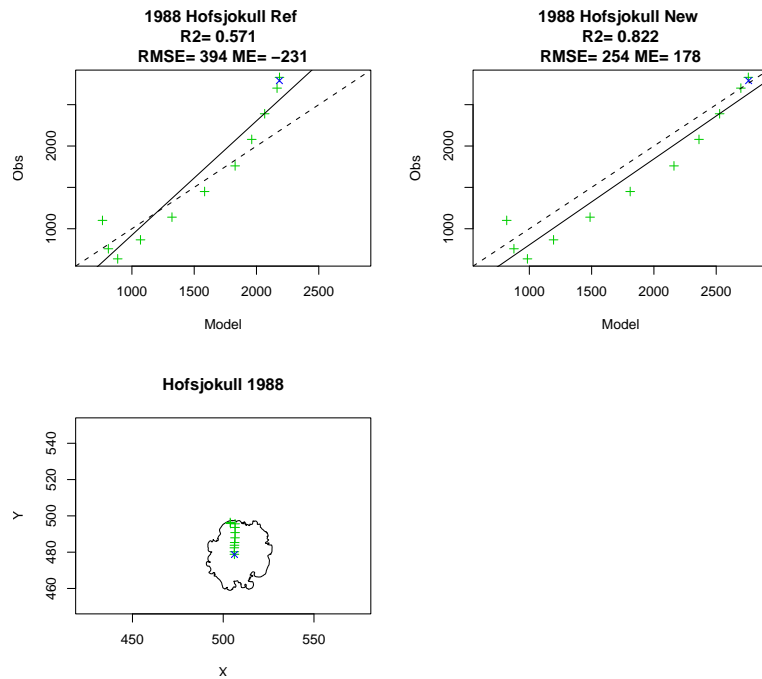


Figure II.1. Winter precipitation on Hofsjökull (1987–1988) simulated with the reference model version (top-left) and the new model version (top-right) at snowstakes (bottom).

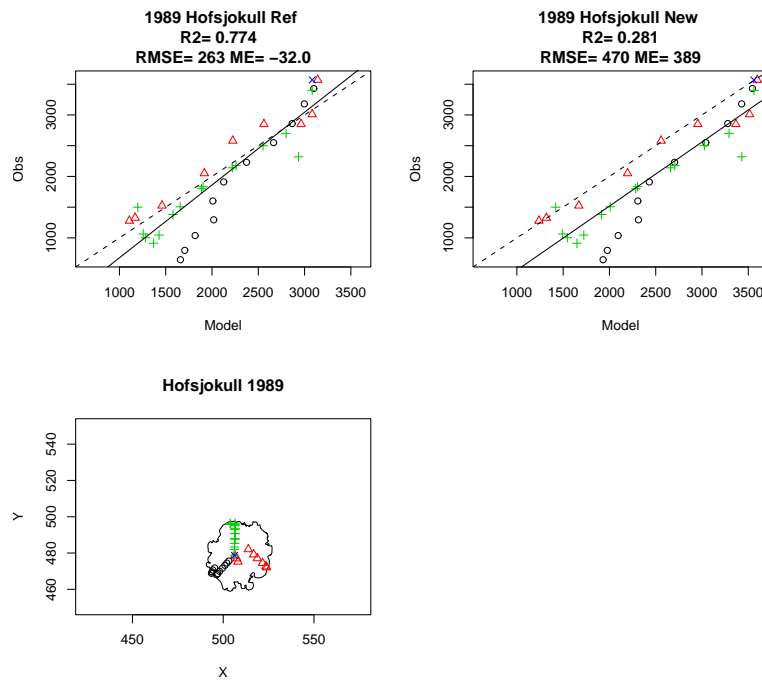


Figure II.2. Winter precipitation on Hofsjökull (1988–1989) simulated with the reference model version (top-left) and the new model version (top-right) at snowstakes (bottom).

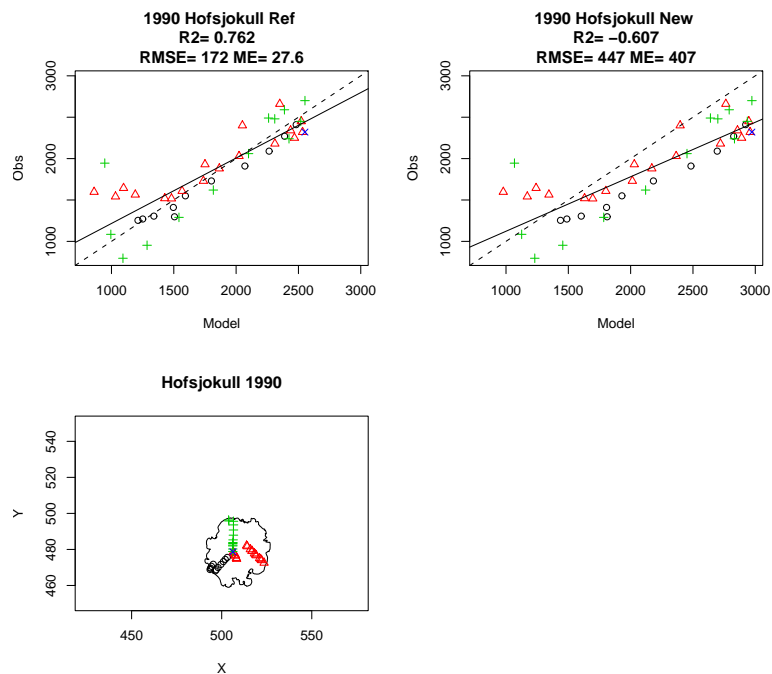


Figure II.3. Winter precipitation on Hofsjökull (1989–1990) simulated with the reference model version (top-left) and the new model version (top-right) at snowstakes (bottom).

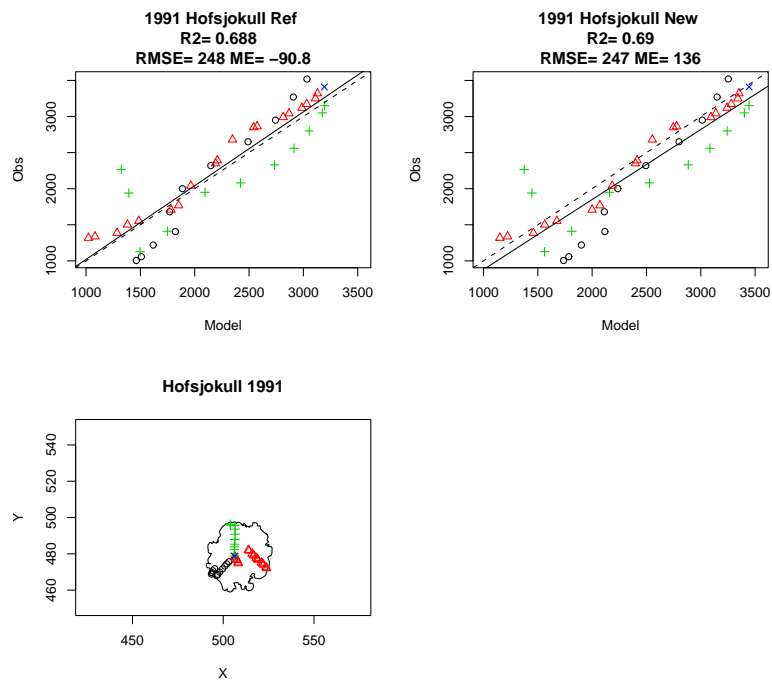


Figure II.4. Winter precipitation on Hofsjökull (1990–1991) simulated with the reference model version (top-left) and the new model version (top-right) at snowstakes (bottom).

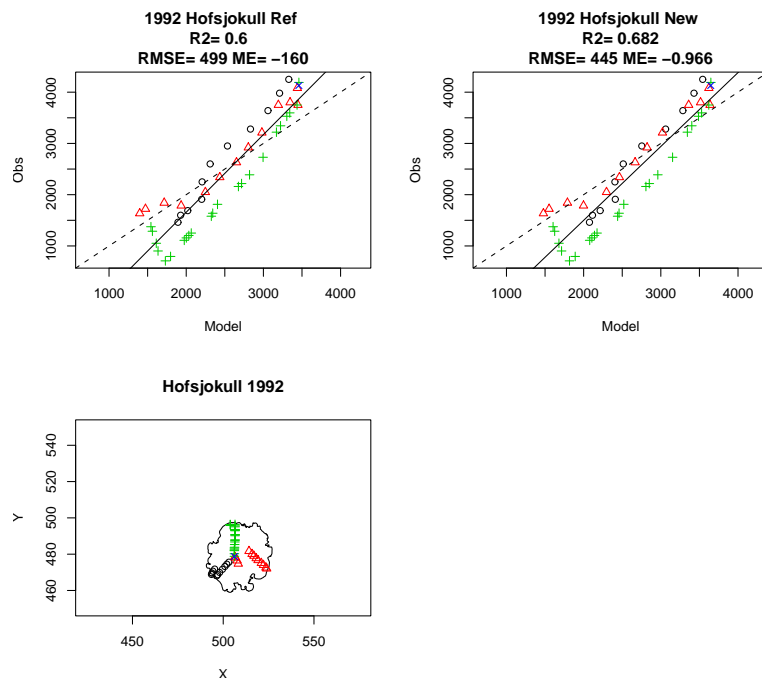


Figure II.5. Winter precipitation on Hofsjökull (1991–1992) simulated with the reference model version (top-left) and the new model version (top-right) at snowstakes (bottom).

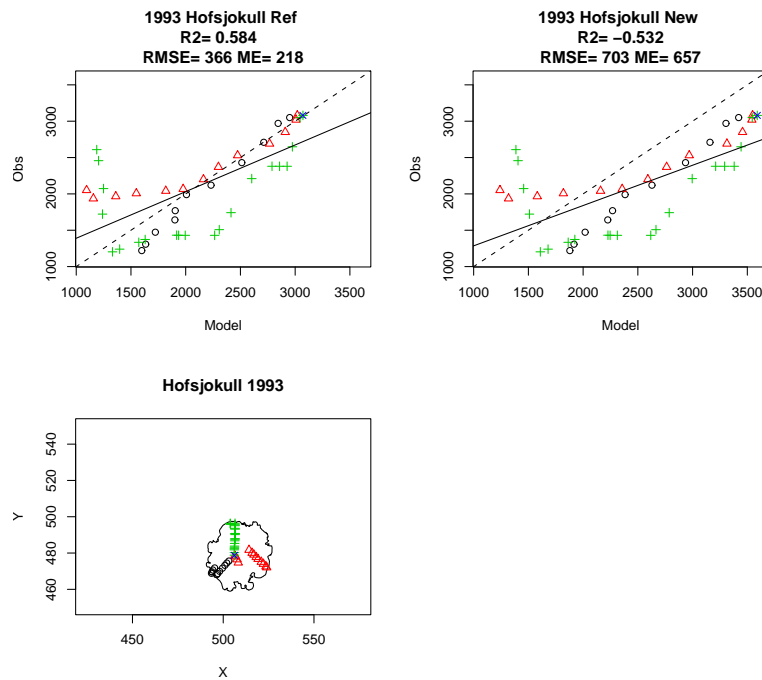


Figure II.6. Winter precipitation on Hofsjökull (1992–1993) simulated with the reference model version (top-left) and the new model version (top-right) at snowstakes (bottom).

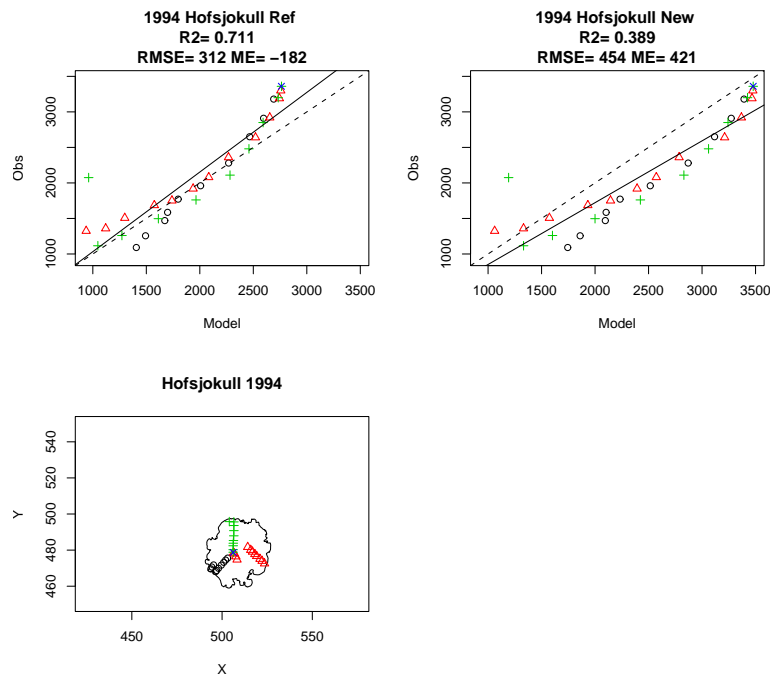


Figure II.7. Winter precipitation on Hofsjökull (1993–1994) simulated with the reference model version (top-left) and the new model version (top-right) at snowstakes (bottom).

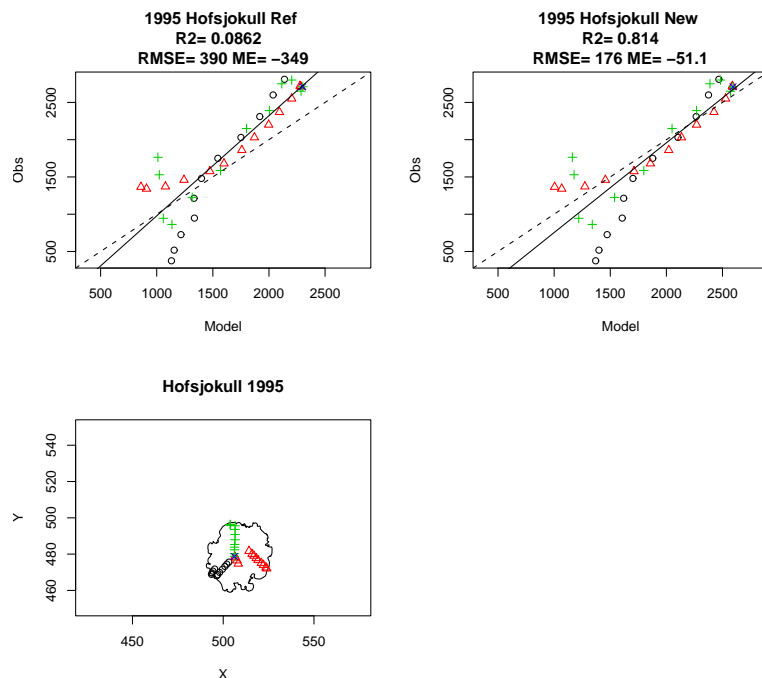


Figure II.8. Winter precipitation on Hofsjökull (1994–1995) simulated with the reference model version (top-left) and the new model version (top-right) at snowstakes (bottom).

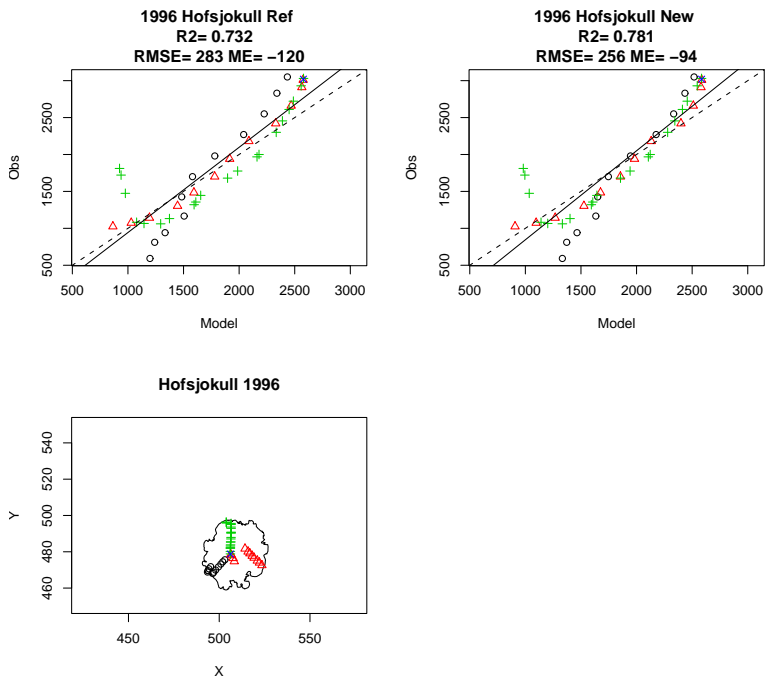


Figure II.9. Winter precipitation on Hofsjökull (1995–1996) simulated with the reference model version (top-left) and the new model version (top-right) at snowstakes (bottom).

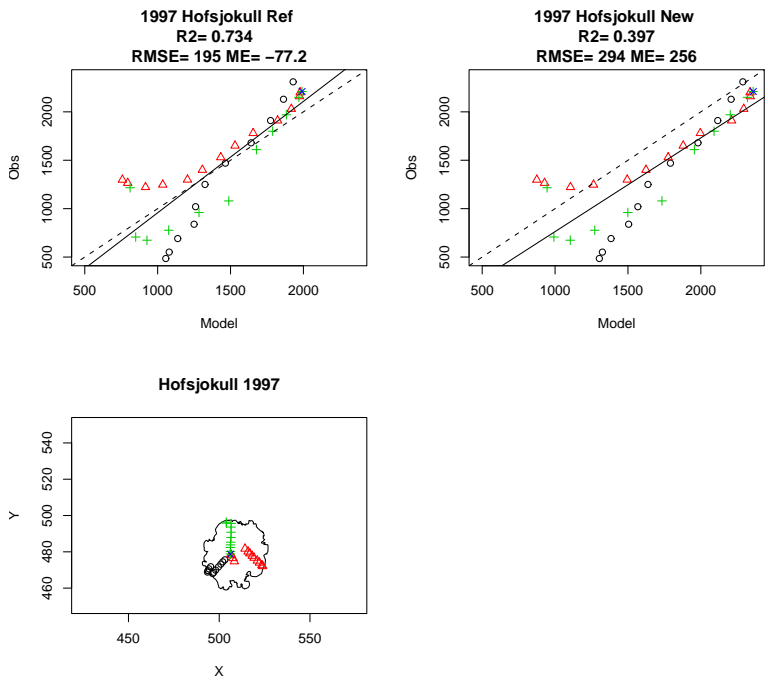


Figure II.10. Winter precipitation on Hofsjökull (1996–1997) simulated with the reference model version (top-left) and the new model version (top-right) at snowstakes (bottom).

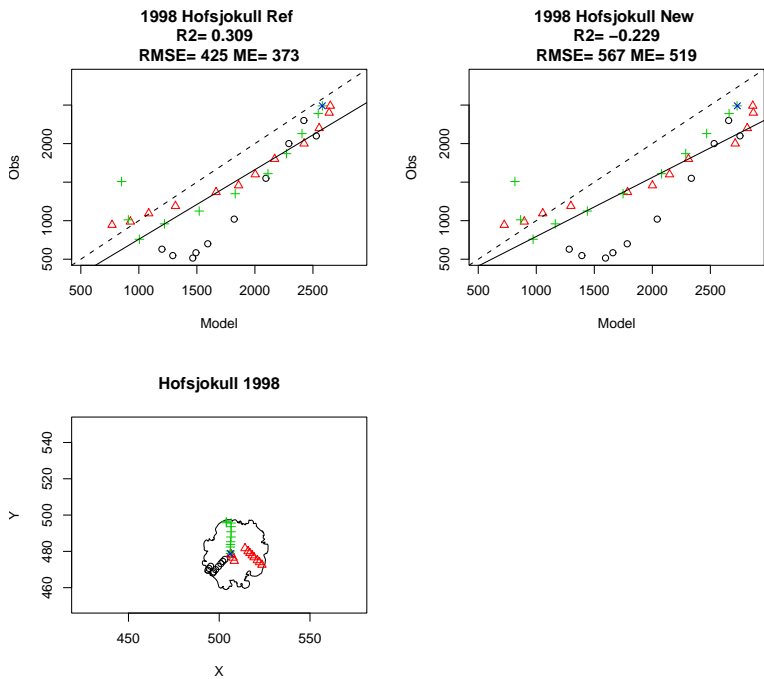


Figure II.11. Winter precipitation on Hofsjökull (1997–1998) simulated with the reference model version (top-left) and the new model version (top-right) at snowstakes (bottom).

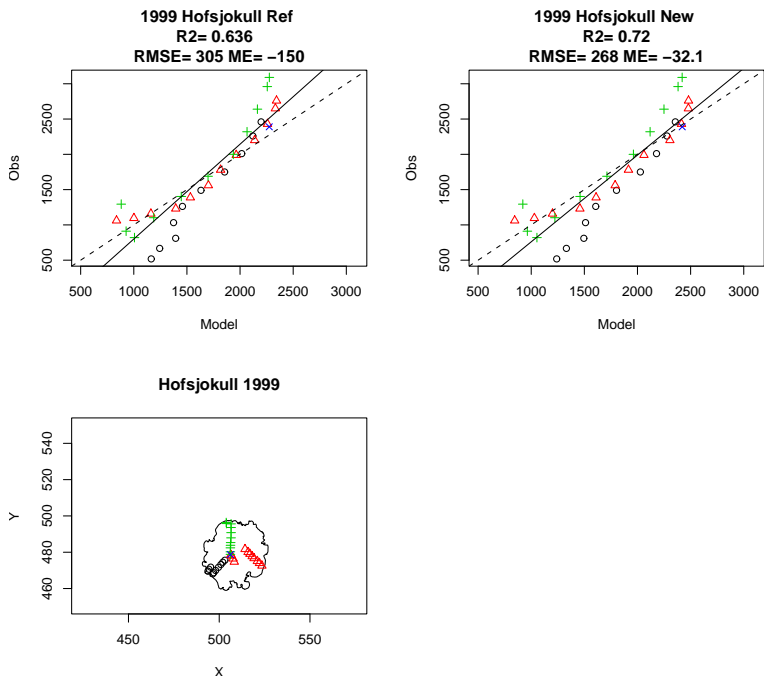


Figure II.12. Winter precipitation on Hofsjökull (1998–1999) simulated with the reference model version (top-left) and the new model version (top-right) at snowstakes (bottom).

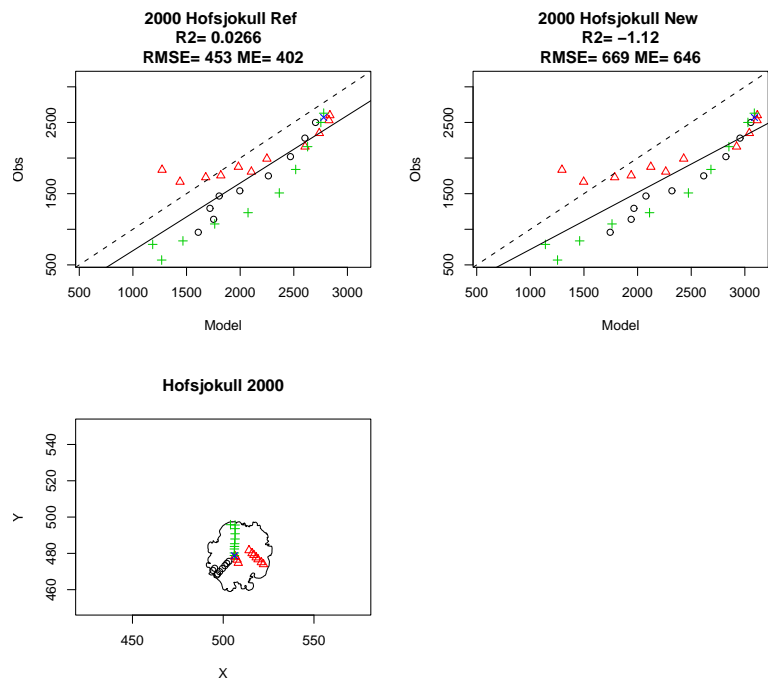


Figure II.13. Winter precipitation on Hofsjökull (1999–2000) simulated with the reference model version (top-left) and the new model version (top-right) at snowstakes (bottom).

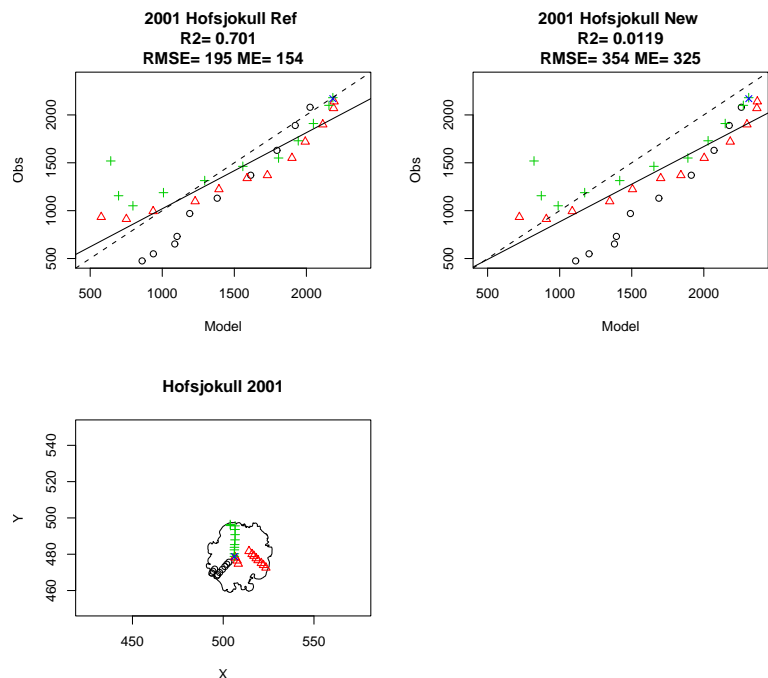


Figure II.14. Winter precipitation on Hofsjökull (2000–2001) simulated with the reference model version (top-left) and the new model version (top-right) at snowstakes (bottom).

III Winter precipitation on Vatnajökull

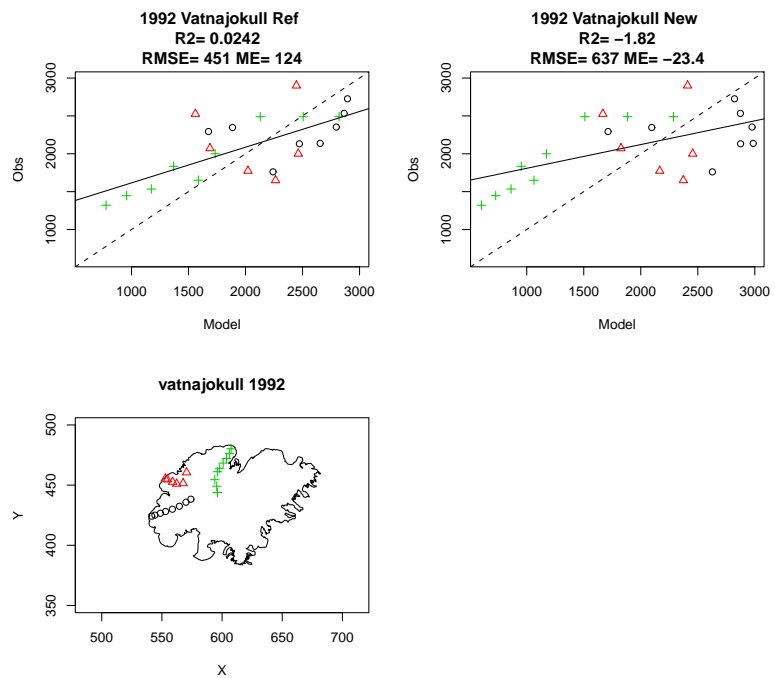


Figure III.1. Winter precipitation on Vatnajökull (1991–1992) simulated with the reference model version (top-left) and the new model version (top-right) at snowstakes (bottom).

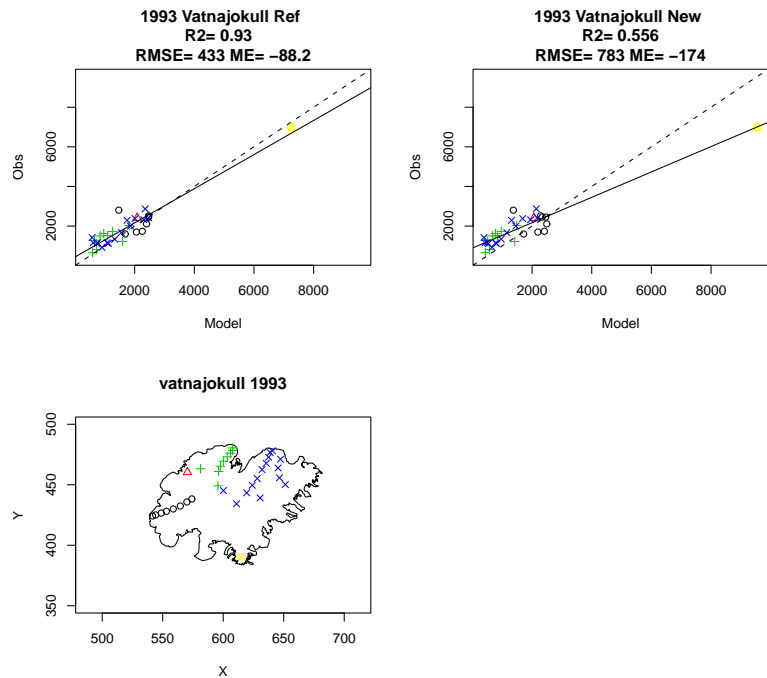


Figure III.2. Winter precipitation on Vatnajökull (1992–1993) simulated with the reference model version (top-left) and the new model version (top-right) at snowstakes (bottom).

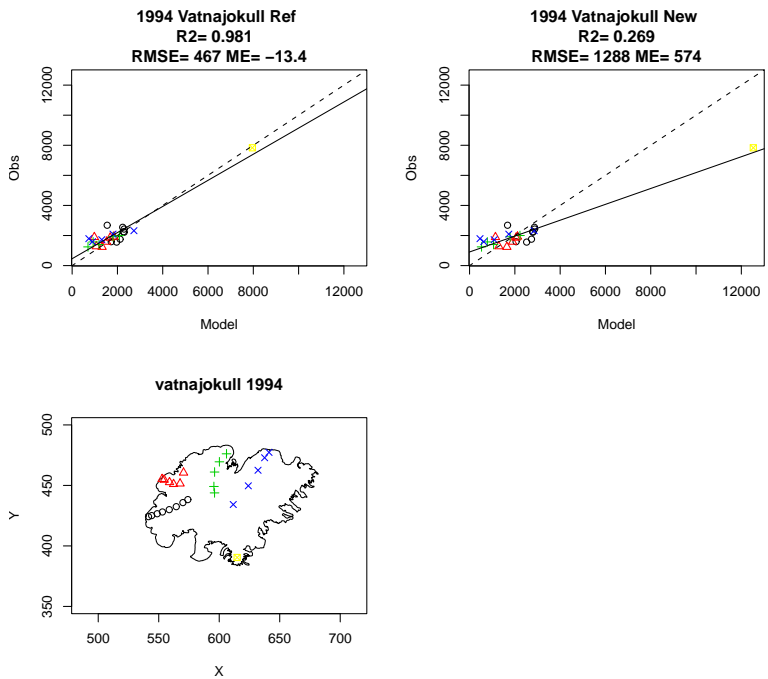


Figure III.3. Winter precipitation on Vatnajökull (1993–1994) simulated with the reference model version (top-left) and the new model version (top-right) at snowstakes (bottom).

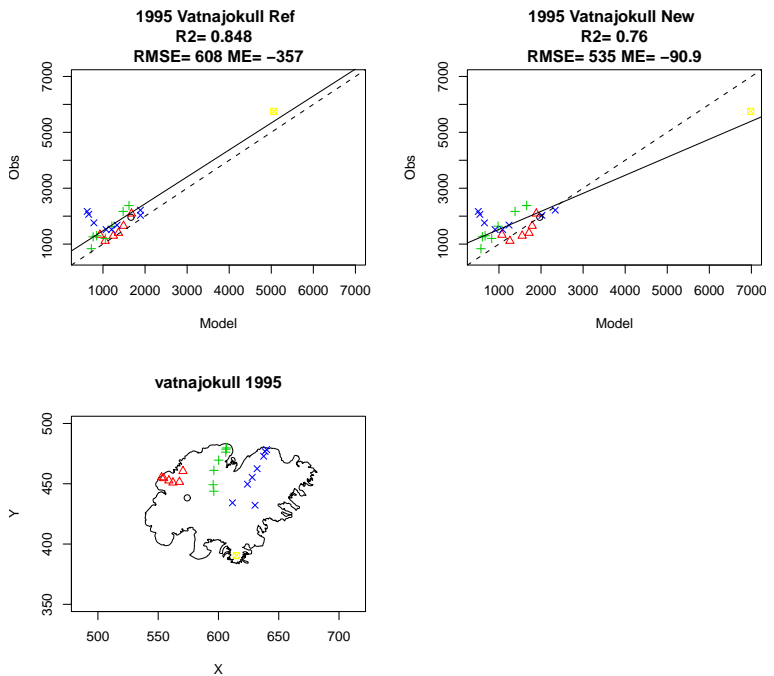


Figure III.4. Winter precipitation on Vatnajökull (1994–1995) simulated with the reference model version (top-left) and the new model version (top-right) at snowstakes (bottom).

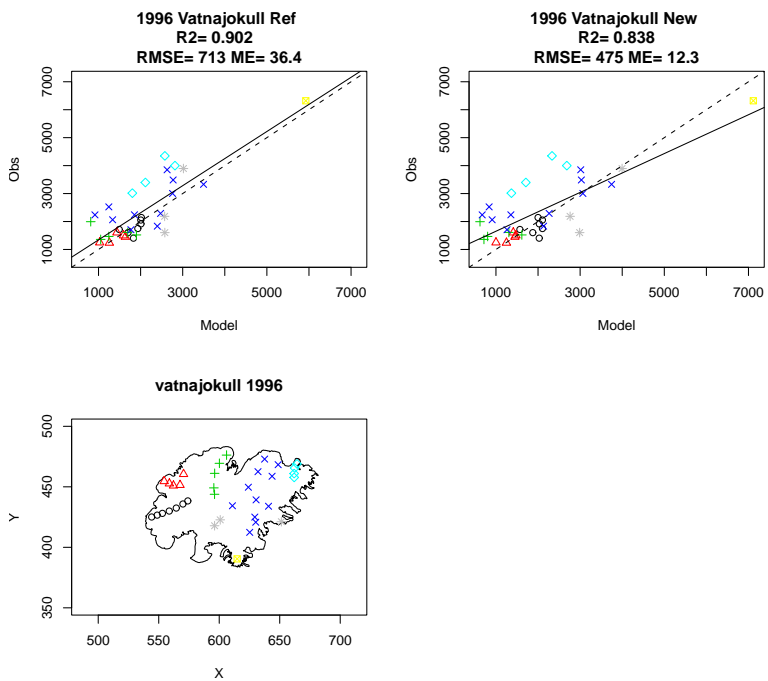


Figure III.5. Winter precipitation on Vatnajökull (1995–1996) simulated with the reference model version (top-left) and the new model version (top-right) at snowstakes (bottom).

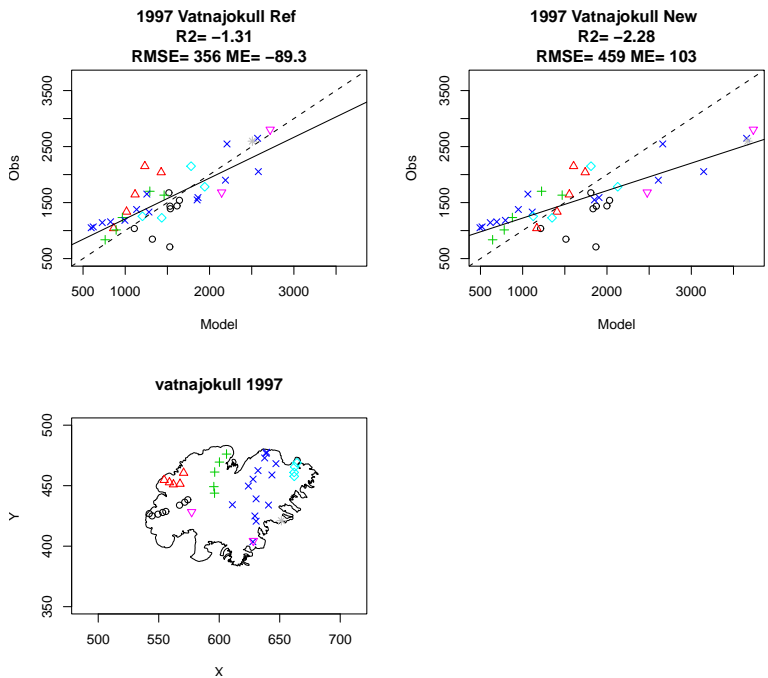


Figure III.6. Winter precipitation on Vatnajökull (1996–1997) simulated with the reference model version (top-left) and the new model version (top-right) at snowstakes (bottom).

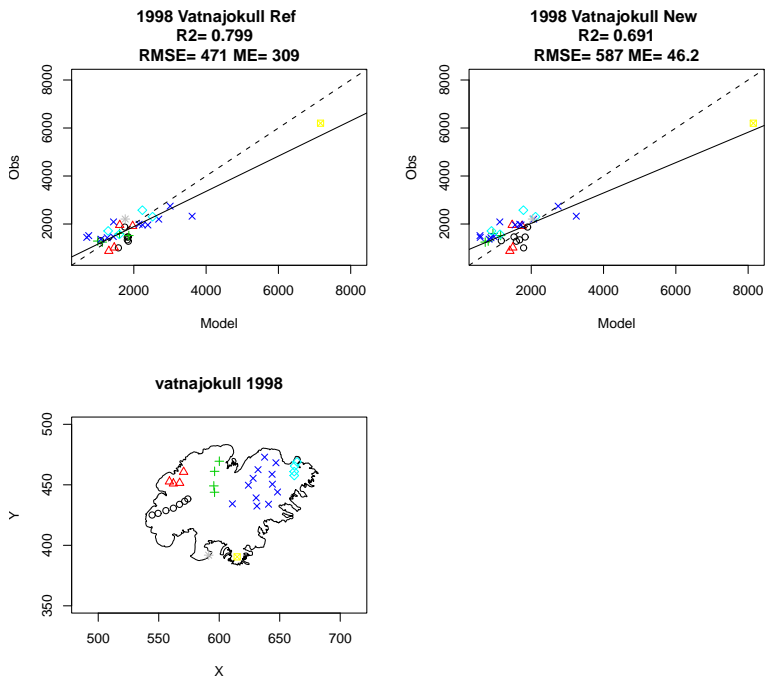


Figure III.7. Winter precipitation on Vatnajökull (1997–1998) simulated with the reference model version (top-left) and the new model version (top-right) at snowstakes (bottom).

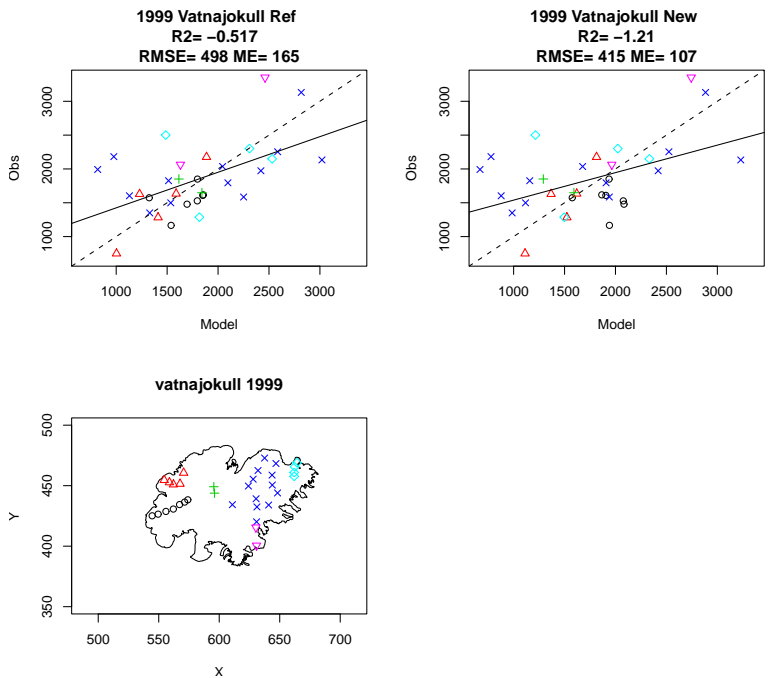


Figure III.8. Winter precipitation on Vatnajökull (1998–1999) simulated with the reference model version (top-left) and the new model version (top-right) at snowstakes (bottom).

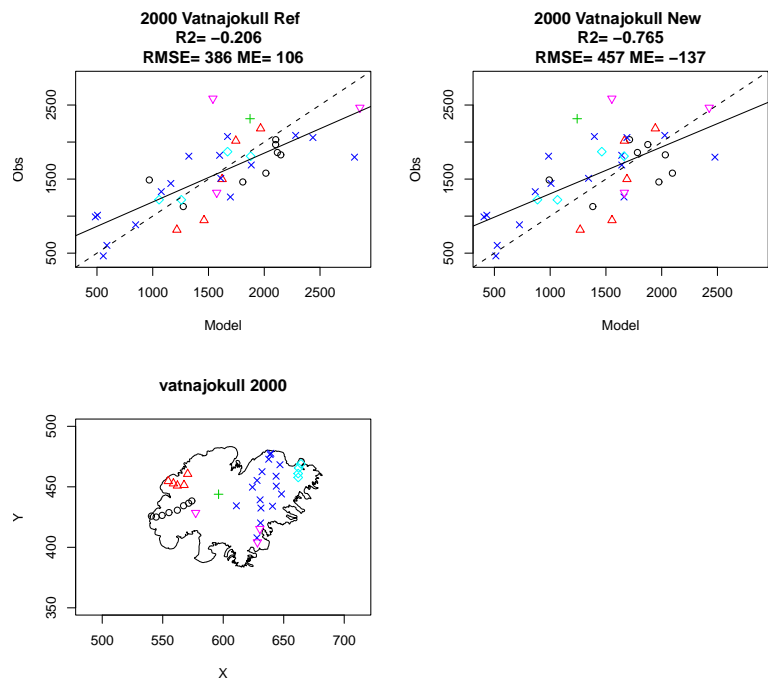


Figure III.9. Winter precipitation on Vatnajökull (1999–2000) simulated with the reference model version (top-left) and the new model version (top-right) at snowstakes (bottom).

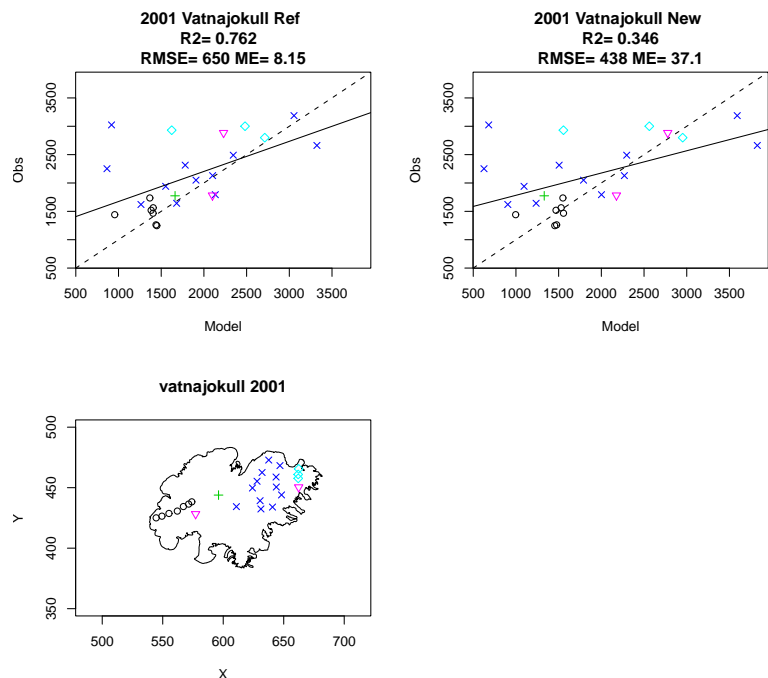


Figure III.10. Winter precipitation on Vatnajökull (2000–2001) simulated with the reference model version (top-left) and the new model version (top-right) at snowstakes (bottom).

IV Winter precipitation on Langjökull

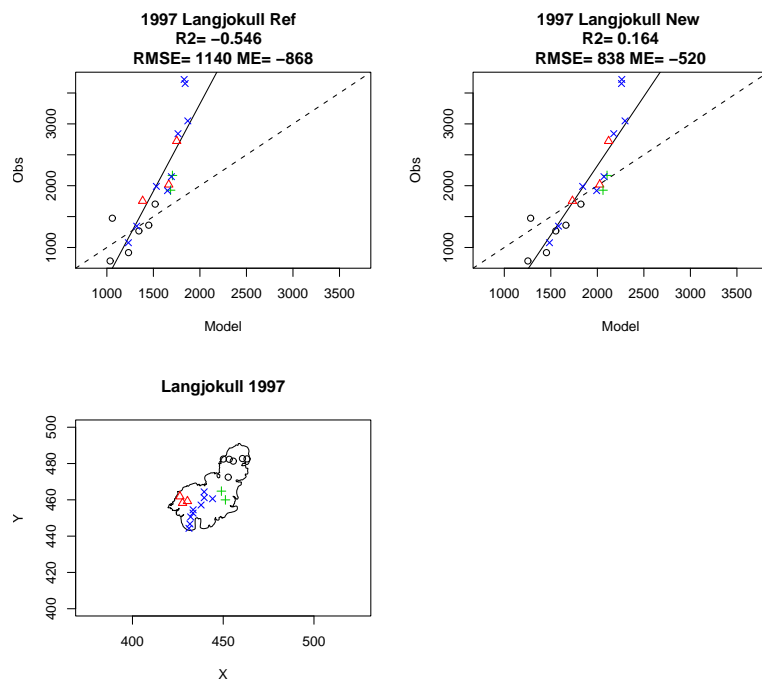


Figure IV.1. Winter precipitation on Langjökull (1996–1997) simulated with the reference model version (top-left) and the new model version (top-right) at snowstakes (bottom).

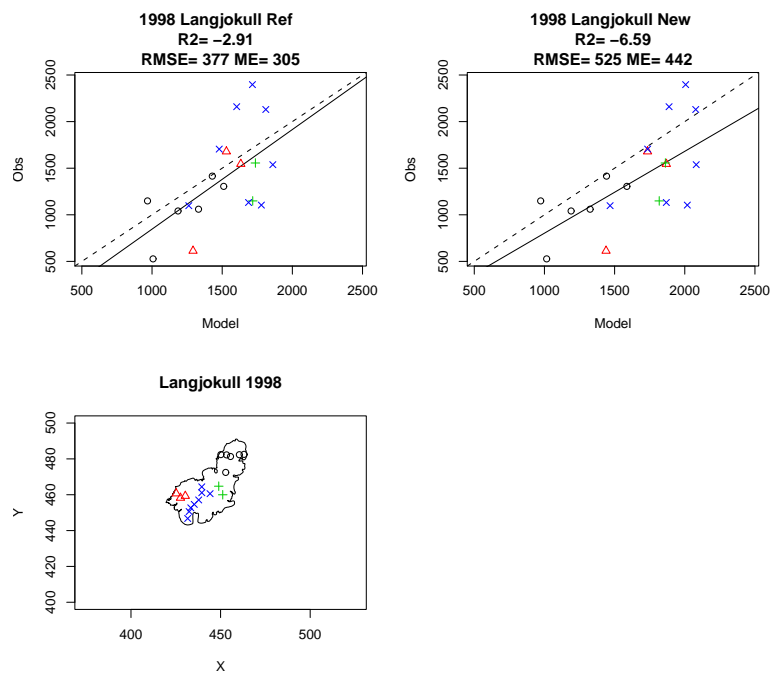


Figure IV.2. Winter precipitation on Langjökull (1997–1998) simulated with the reference model version (top-left) and the new model version (top-right) at snowstakes (bottom).

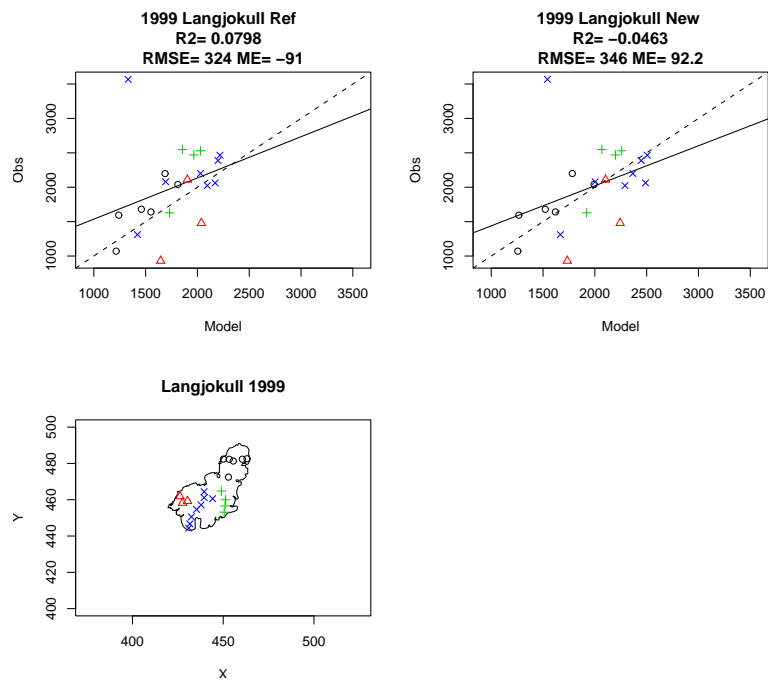


Figure IV.3. Winter precipitation on Langjökull (1998–1999) simulated with the reference model version (top-left) and the new model version (top-right) at snowstakes (bottom).

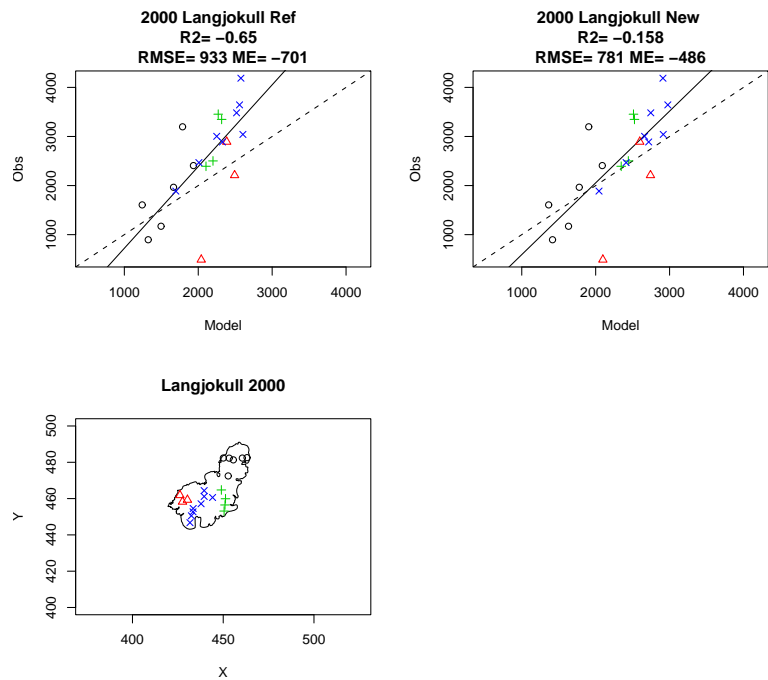


Figure IV.4. Winter precipitation on Langjökull (1999–2000) simulated with the reference model version (top-left) and the new model version (top-right) at snowstakes (bottom).

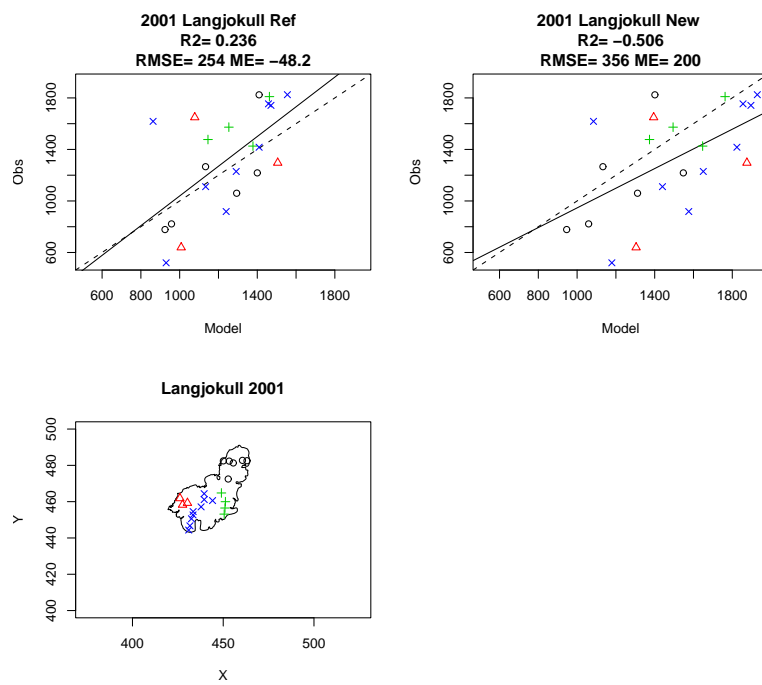


Figure IV.5. Winter precipitation on Langjökull (2000–2001) simulated with the reference model version (top-left) and the new model version (top-right) at snowstakes (bottom).

V Statistical characteristics of daily precipitation (1991–2000)

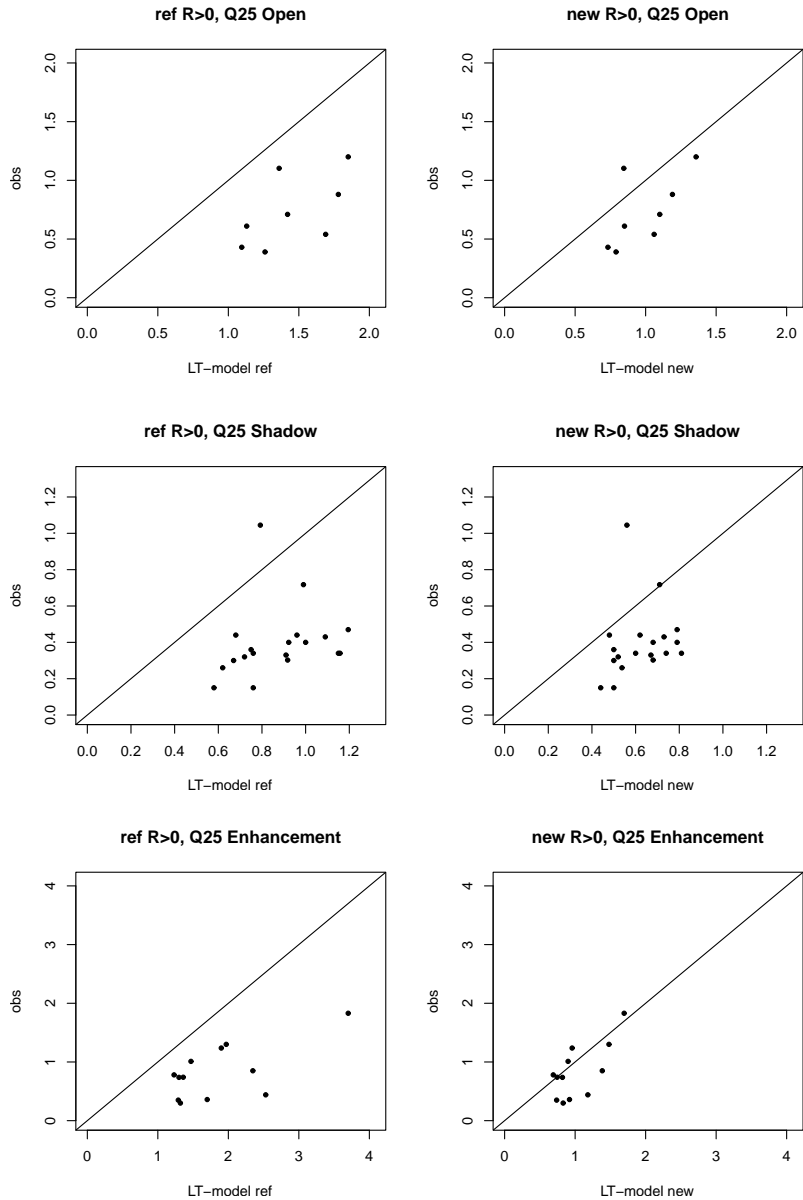


Figure V.1. 25% quantile for strictly positive daily precipitation at stations located in open terrain (top) rain-shadow terrain (middle) and windward terrain (bottom), simulated with the reference model version (left) and the new model version (right).

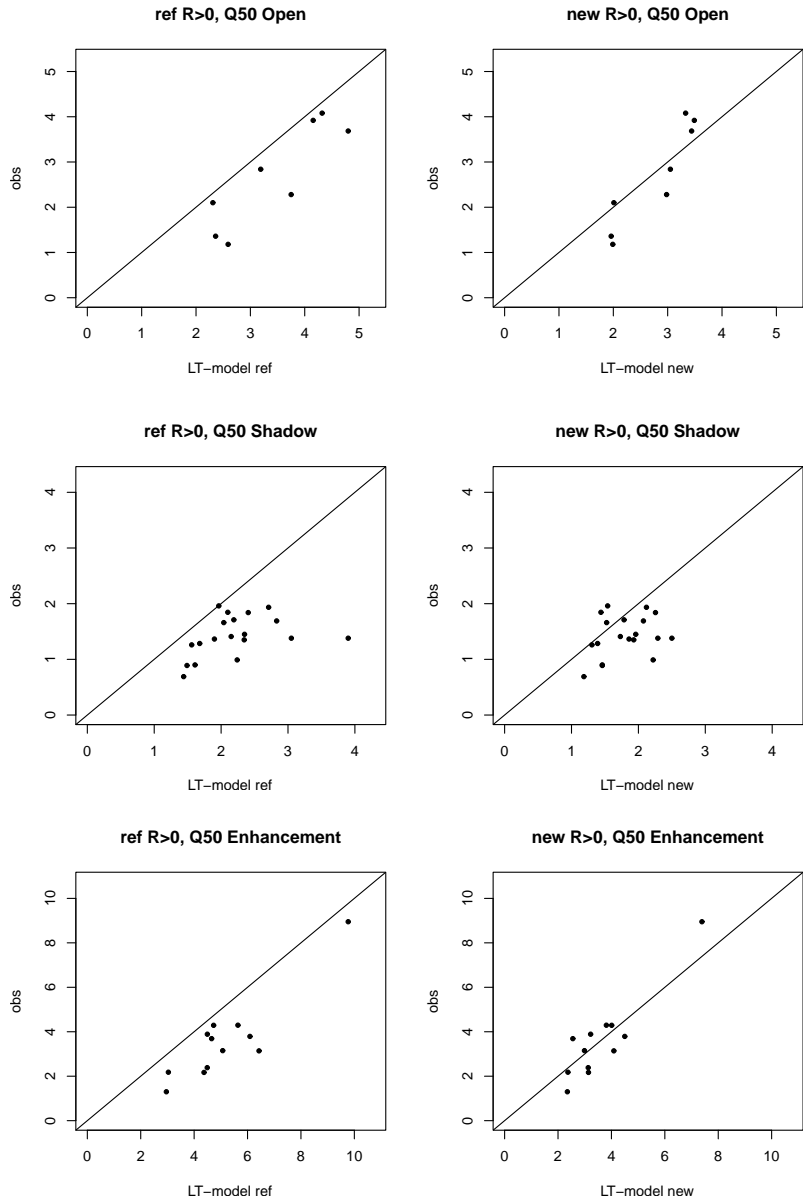


Figure V.2. 50% quantile for strictly positive daily precipitation at stations located in open terrain (top) rain-shadow terrain (middle) and windward terrain (bottom), simulated with the reference model version (left) and the new model version (right).

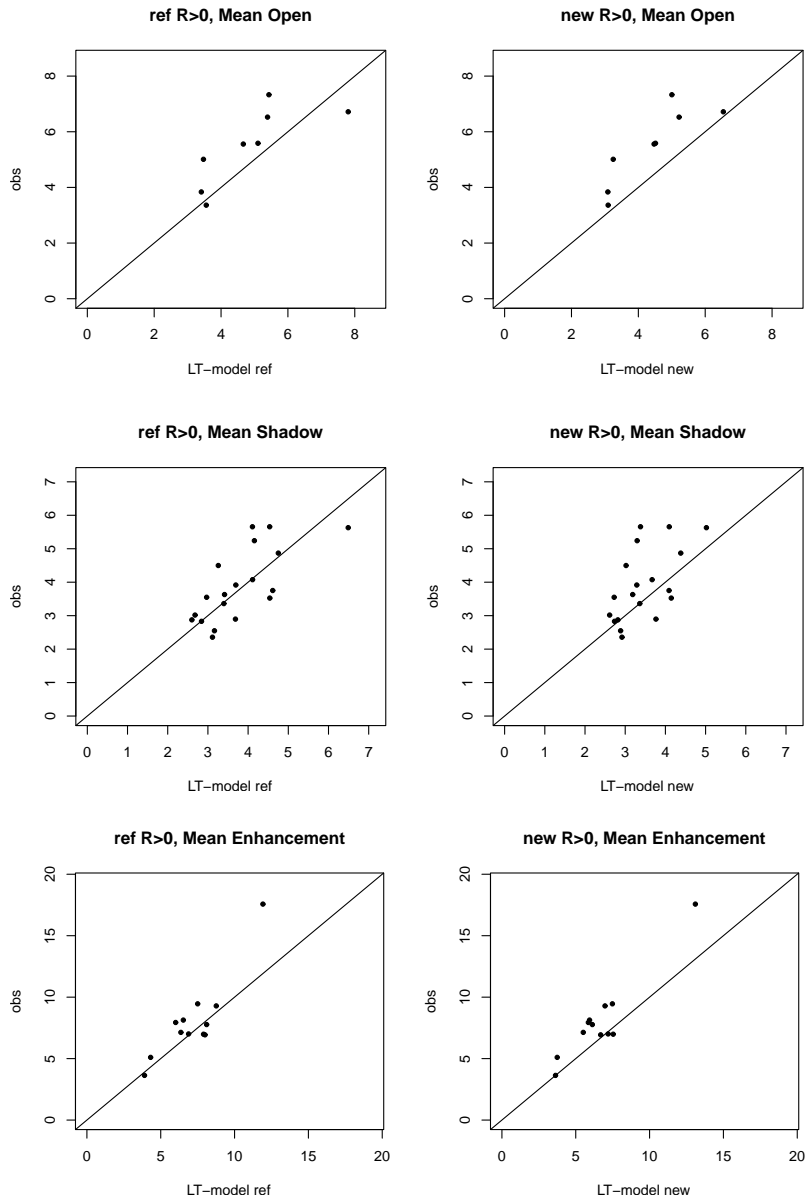


Figure V.3. Mean strictly positive daily precipitation at stations located in open terrain (top) rain-shadow terrain (middle) and windward terrain (bottom), simulated with the reference model version (left) and the new model version (right).

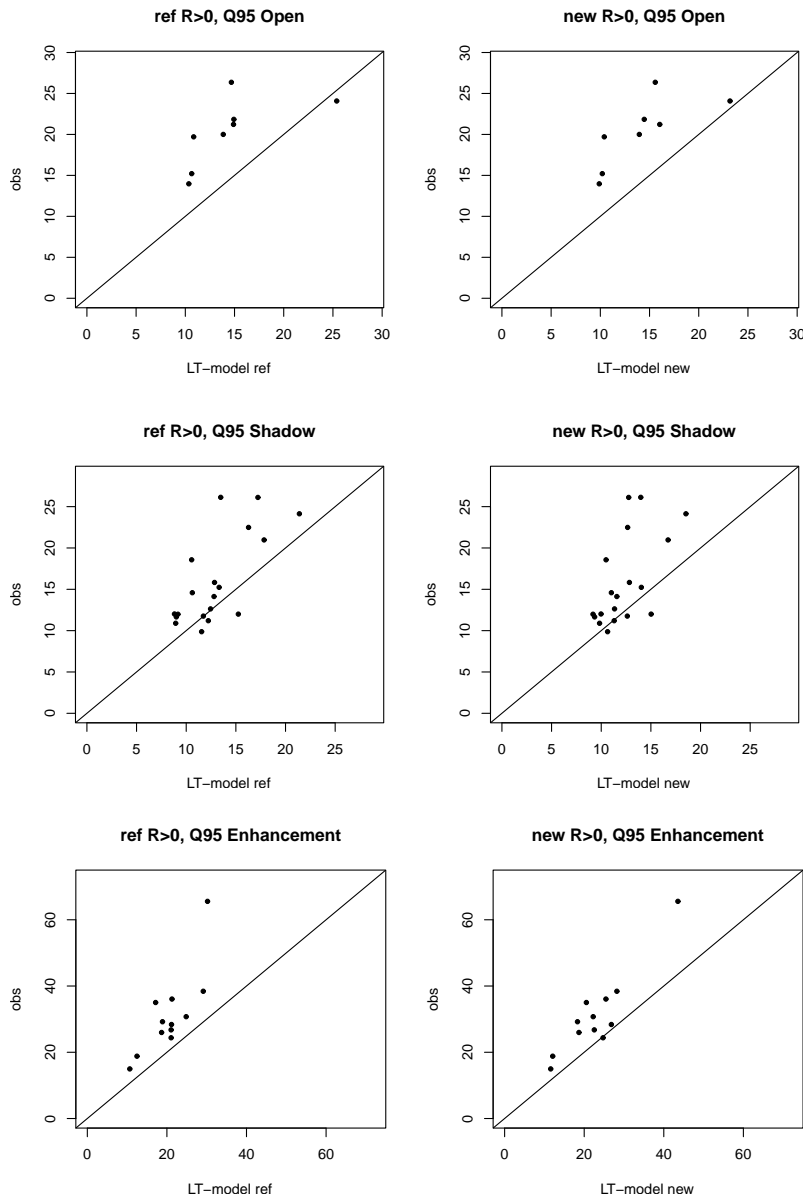


Figure V.4. 95% quantile for strictly positive daily precipitation at stations located in open terrain (top) rain-shadow terrain (middle) and windward terrain (bottom), simulated with the reference model version (left) and the new model version (right).

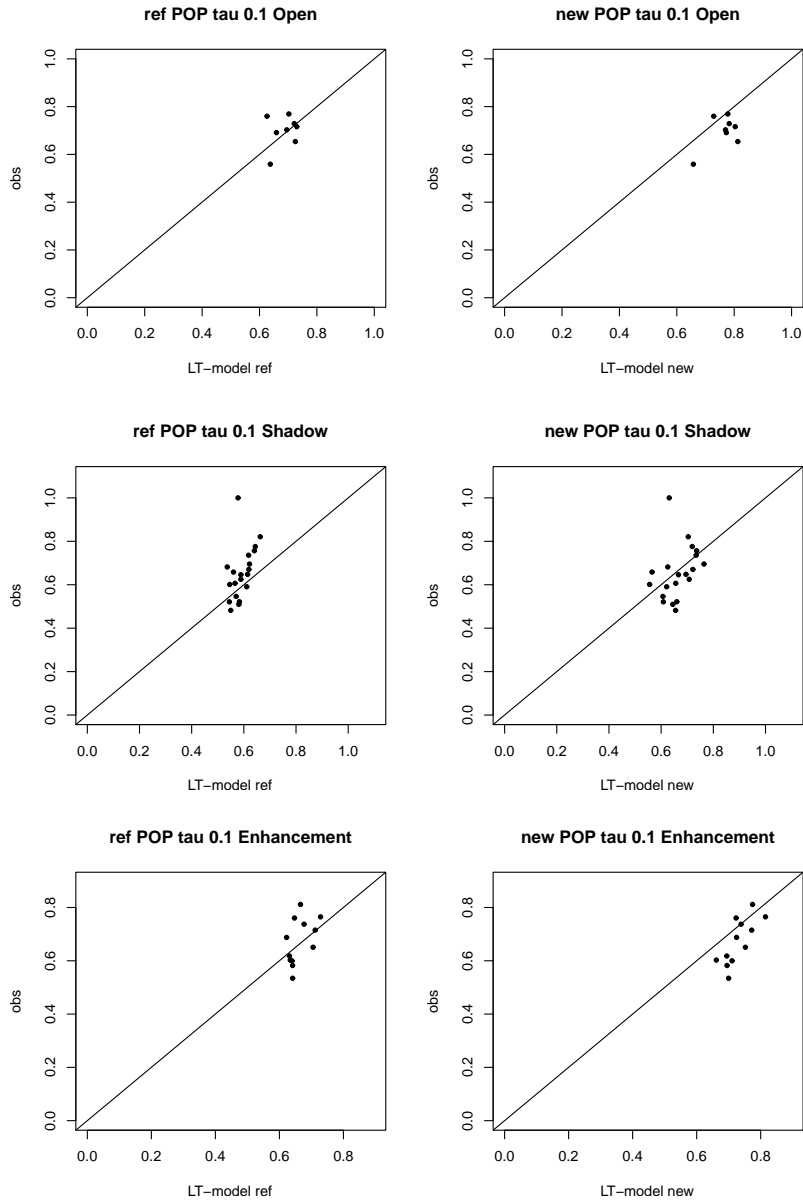


Figure V.5. Probability of Precipitation above 0.1mm/day at stations located in open terrain (top) rain-shadow terrain (middle) and windward terrain (bottom), simulated with the reference model version (left) and the new model version (right).

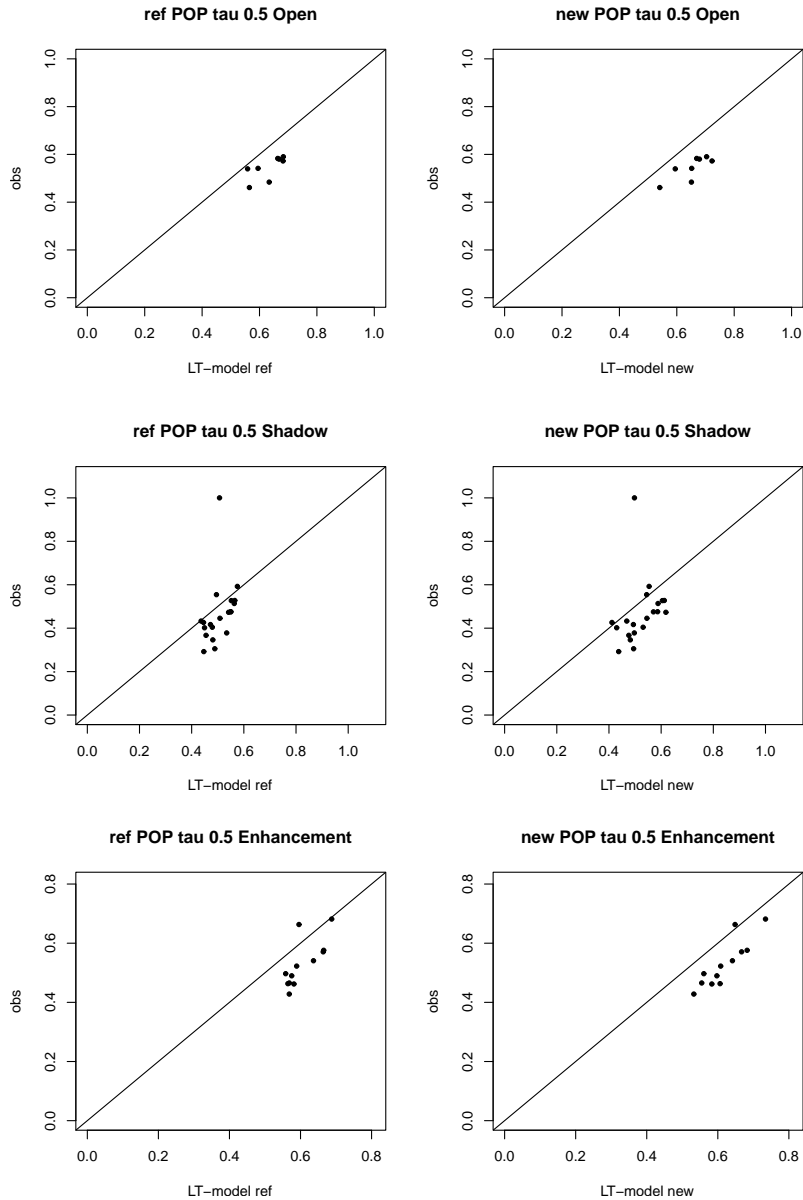


Figure V.6. Probability of Precipitation above 0.5mm/day at stations located in open terrain (top) rain-shadow terrain (middle) and windward terrain (bottom), simulated with the reference model version (left) and the new model version (right).

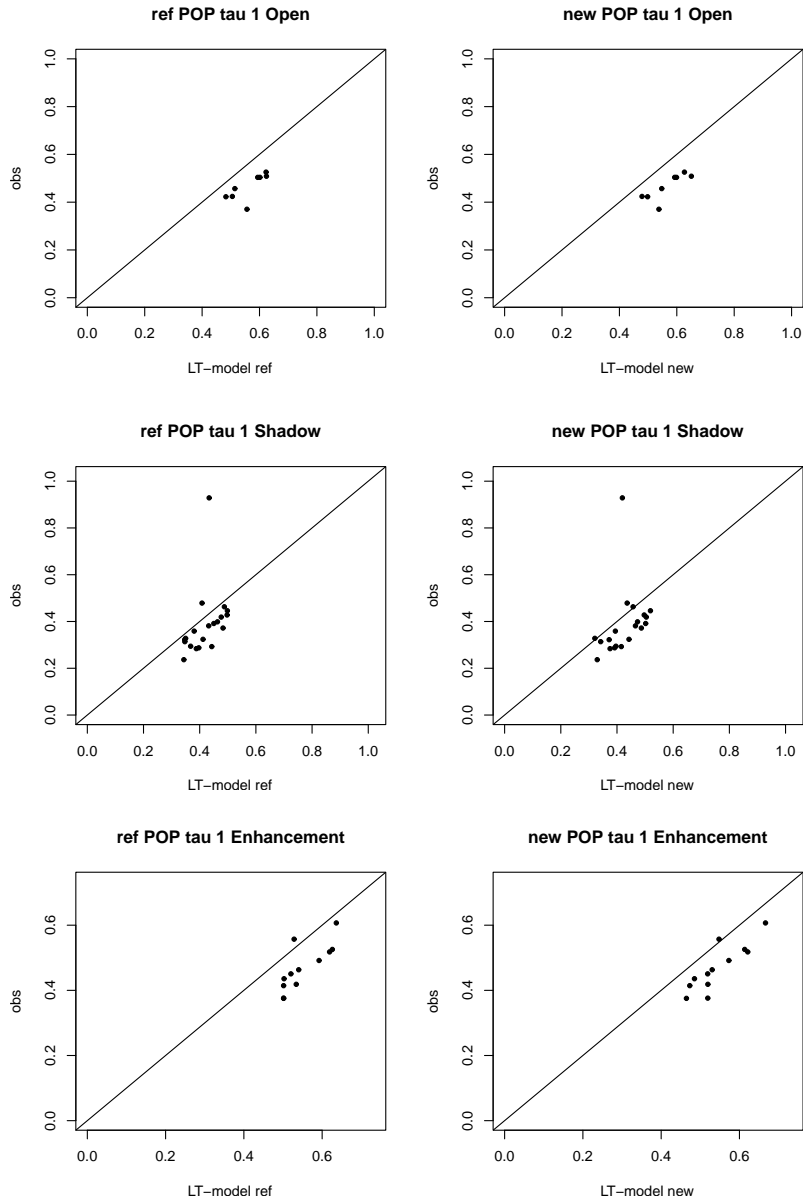


Figure V.7. Probability of Precipitation above 1mm/day at stations located in open terrain (top) rain-shadow terrain (middle) and windward terrain (bottom), simulated with the reference model version (left) and the new model version (right).

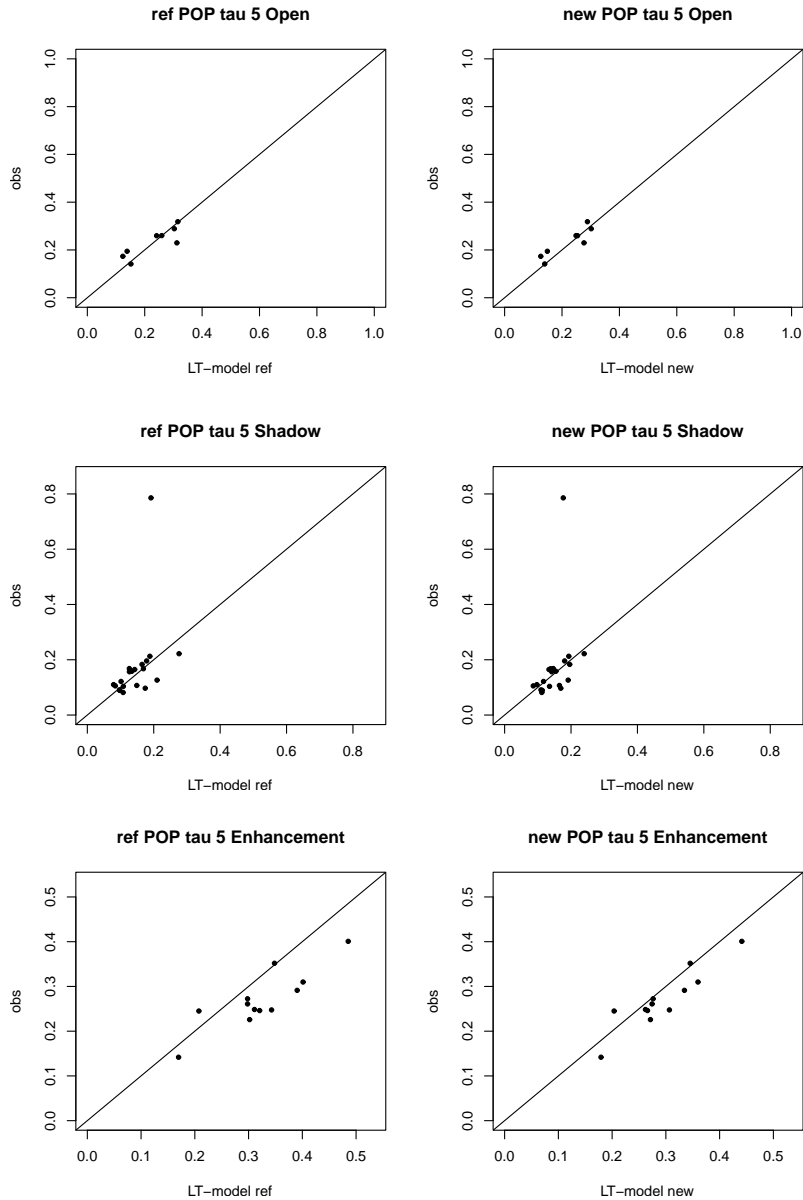


Figure V.8. Probability of Precipitation above 5mm/day at stations located in open terrain (top) rain-shadow terrain (middle) and windward terrain (bottom), simulated with the reference model version (left) and the new model version (right).

VI Annual precipitation maps (1987–2001)

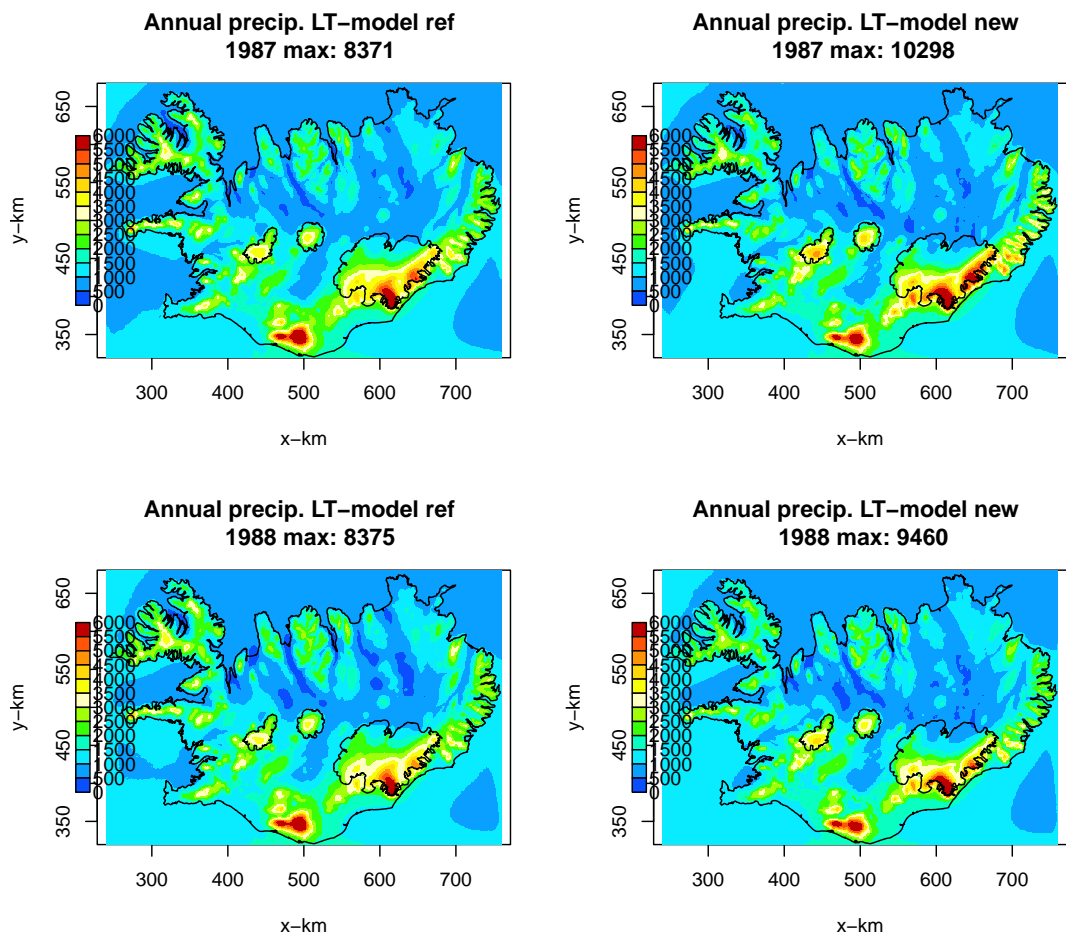


Figure VI.1. Annual precipitation maps in 1987 (top) and 1988 (bottom) simulated with the reference model version (left) and the new model version (right).

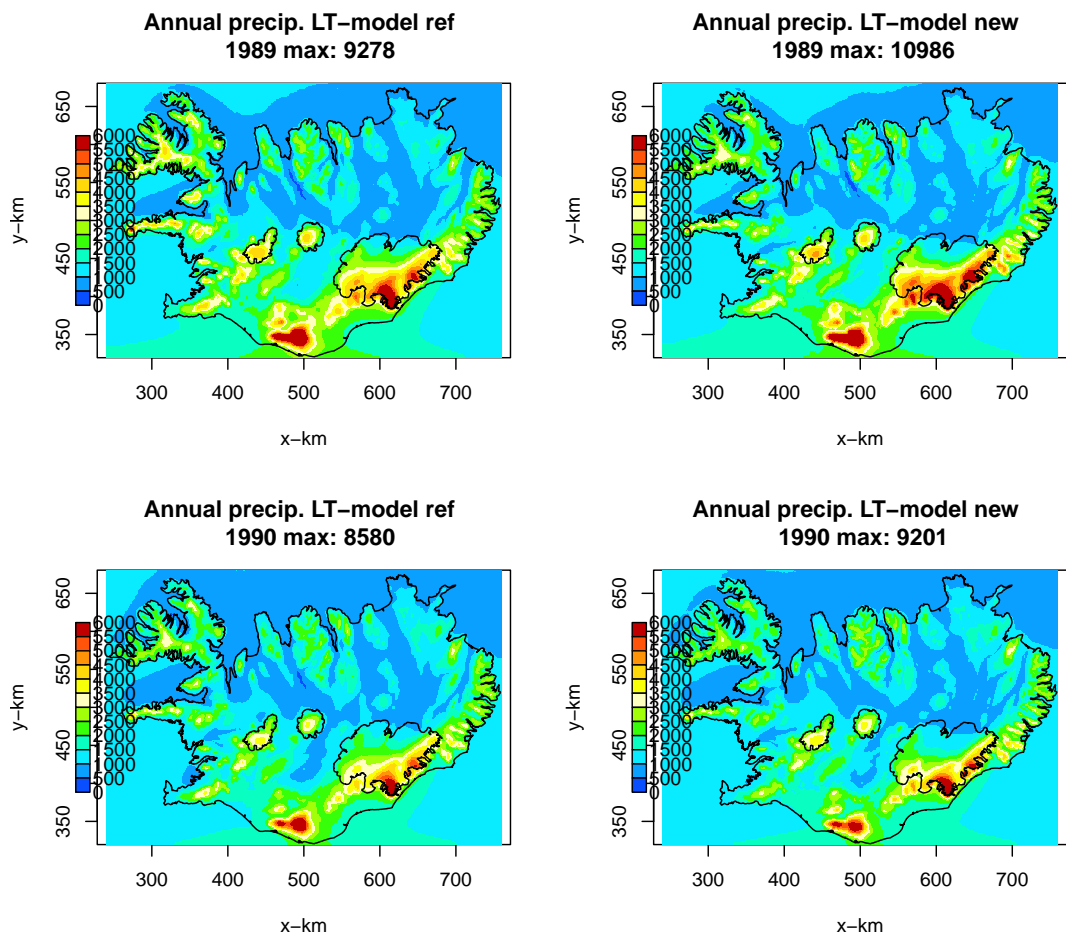


Figure VI.2. Annual precipitation maps in 1989 (top) and 1990 (bottom) simulated with the reference model version (left) and the new model version (right).

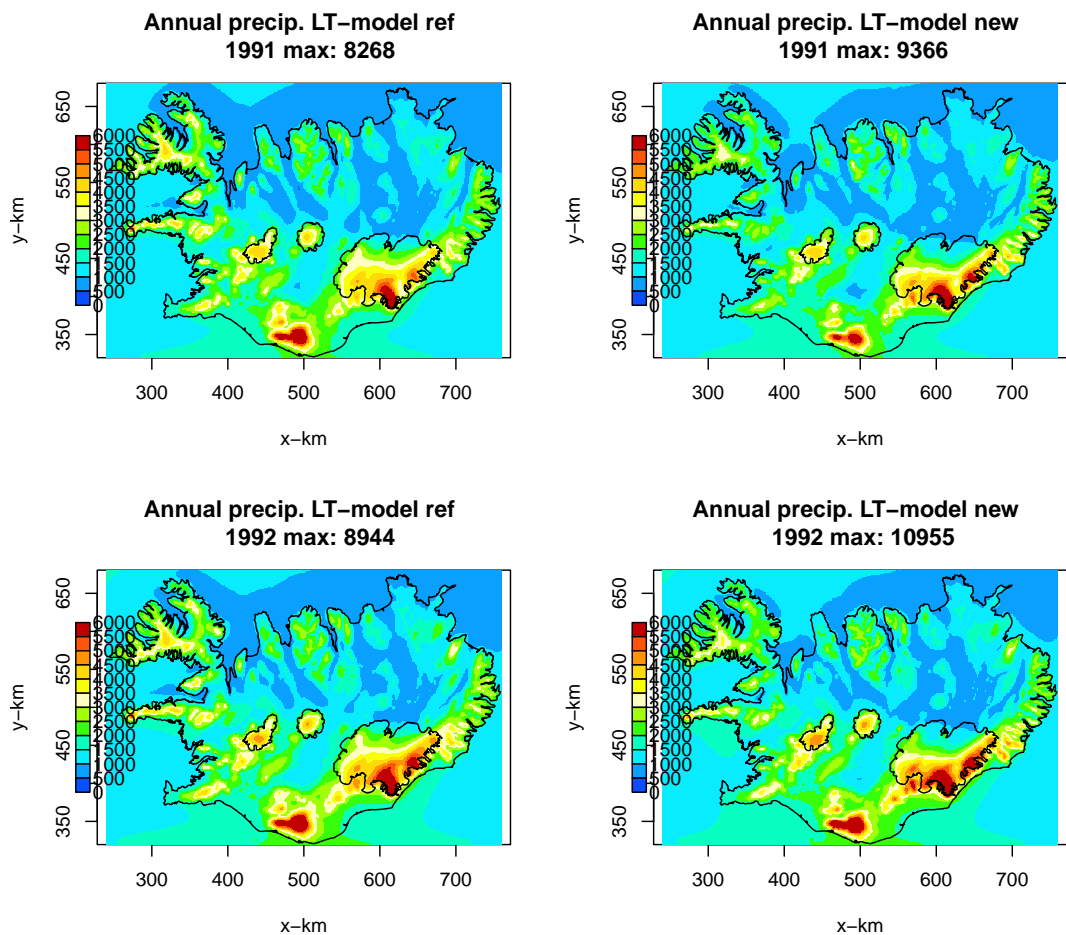


Figure VI.3. Annual precipitation maps in 1991 (top) and 1992 (bottom) simulated with the reference model version (left) and the new model version (right).

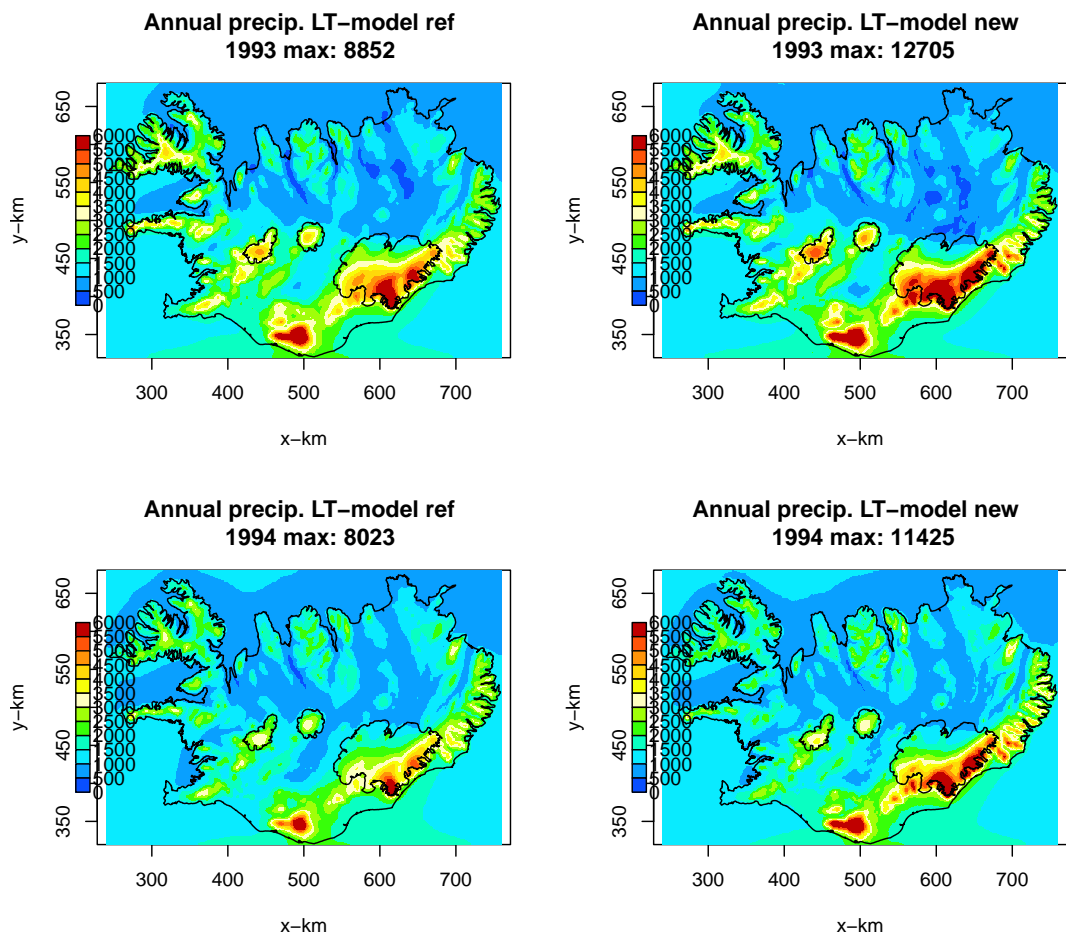


Figure VI.4. Annual precipitation maps in 1993 (top) and 1994 (bottom) simulated with the reference model version (left) and the new model version (right).

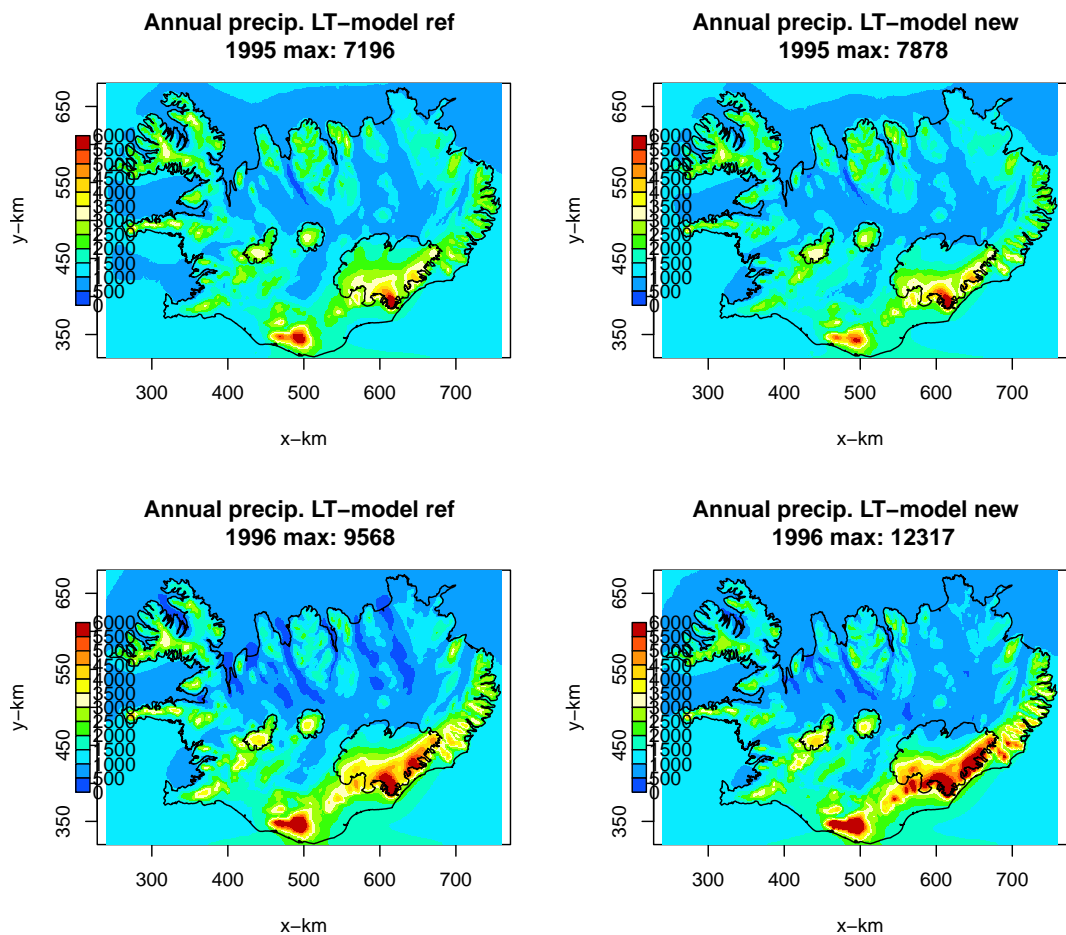


Figure VI.5. Annual precipitation maps in 1995 (top) and 1996 (bottom) simulated with the reference model version (left) and the new model version (right).

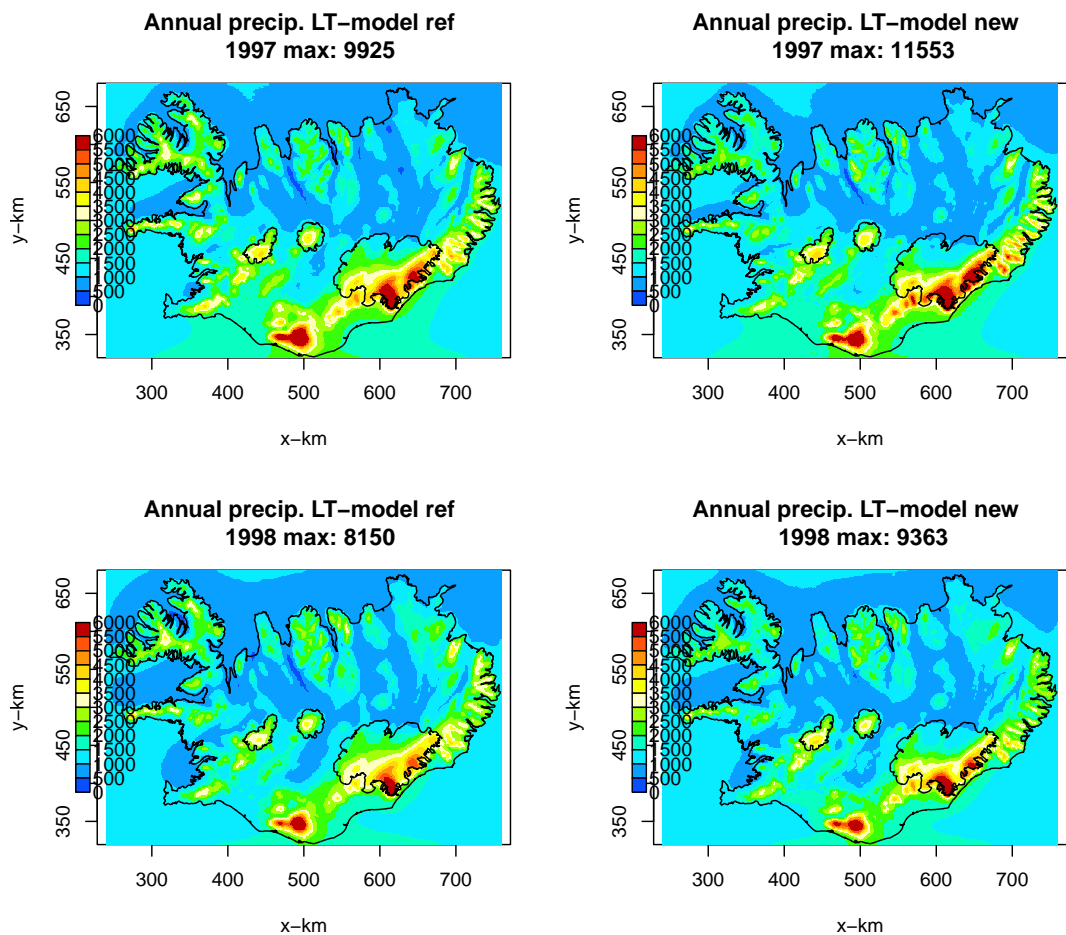


Figure VI.6. Annual precipitation maps in 1997 (top) and 1998 (bottom) simulated with the reference model version (left) and the new model version (right).

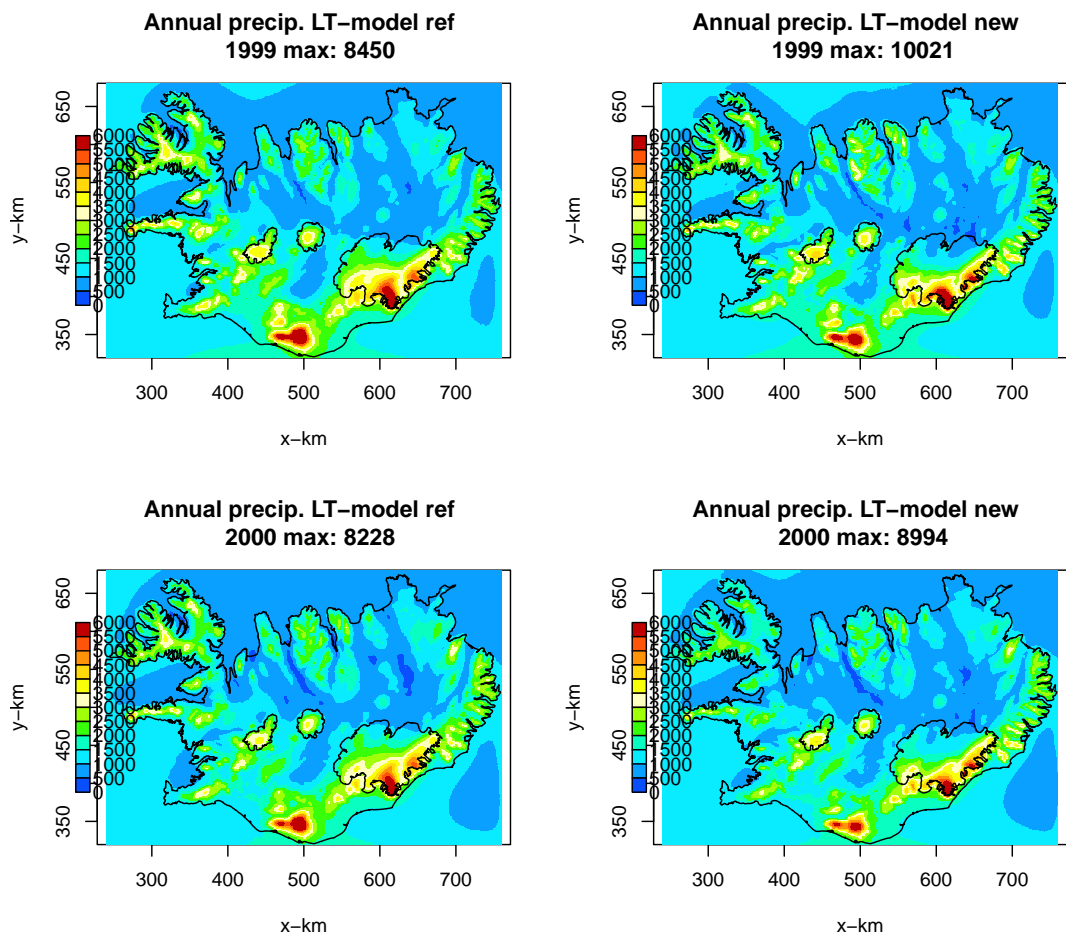


Figure VI.7. Annual precipitation maps in 1999 (top) and 2000 (bottom) simulated with the reference model version (left) and the new model version (right).

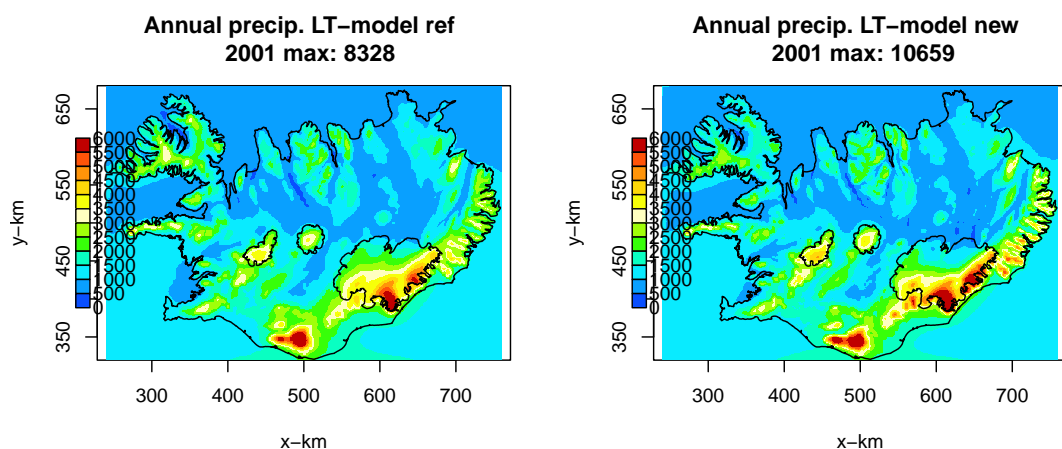


Figure VI.8. Annual precipitation maps in 2001 simulated with the reference model version (left) and the new model version (right).

VII Mean monthly precipitation maps (1987–2001)

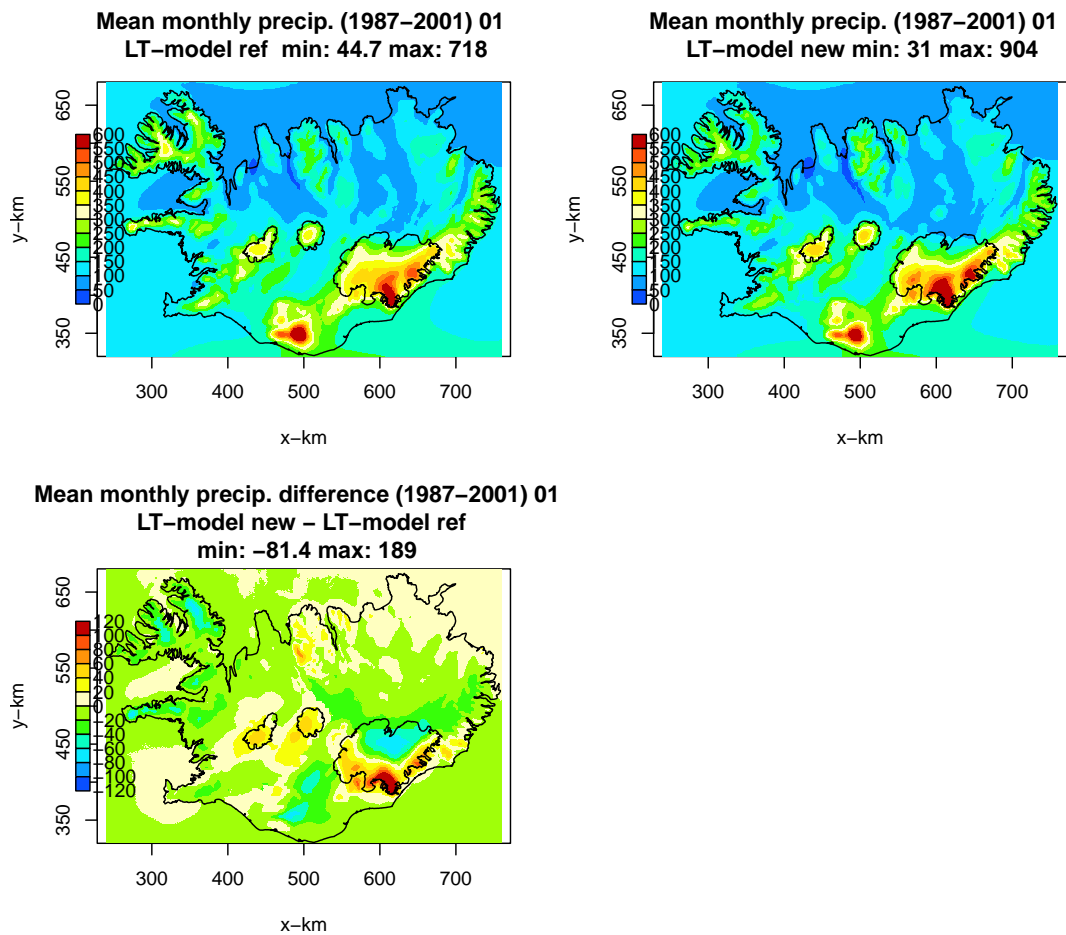


Figure VII.1. Mean January precipitation map (1987–2001) simulated with the reference model version (top-left) and the new model version (top-right), and the difference between the new and reference maps (bottom).

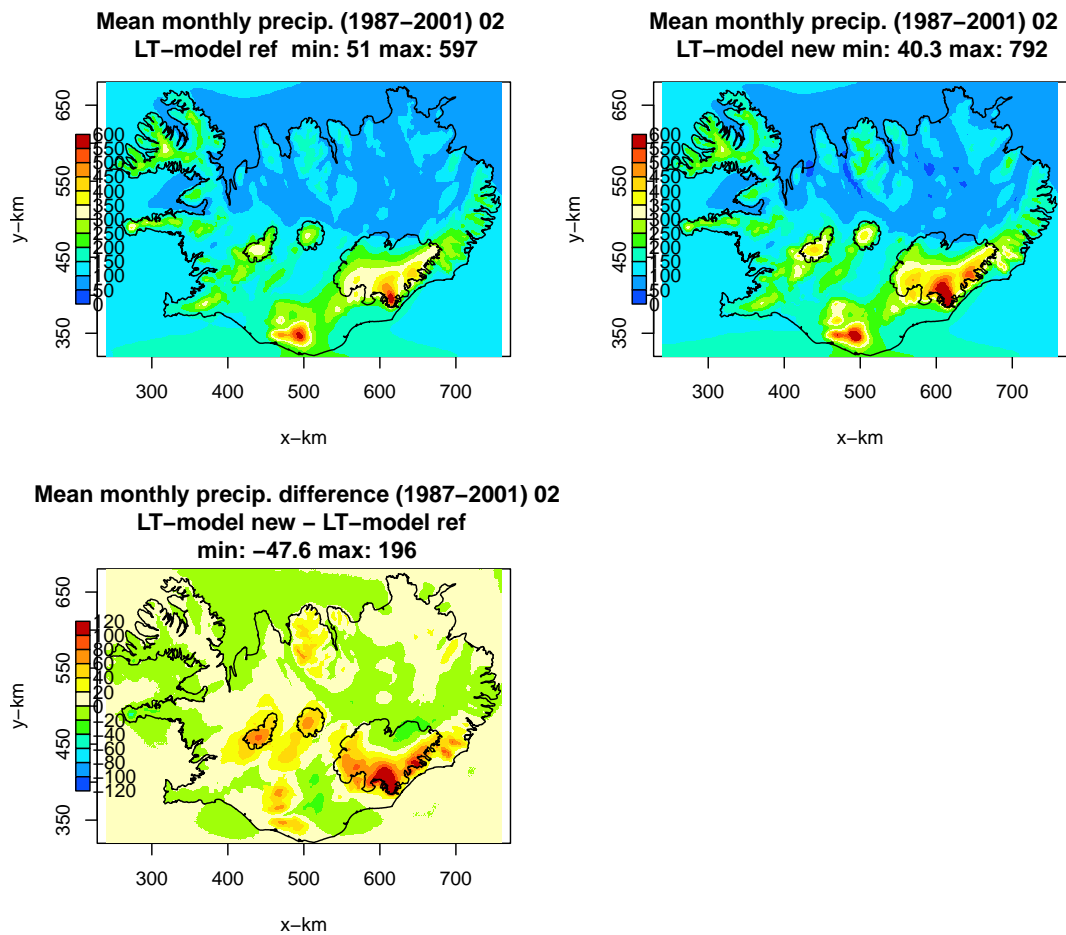


Figure VII.2. Mean February precipitation map (1987–2001) simulated with the reference model version (top-left) and the new model version (top-right), and the difference between the new and reference maps (bottom).

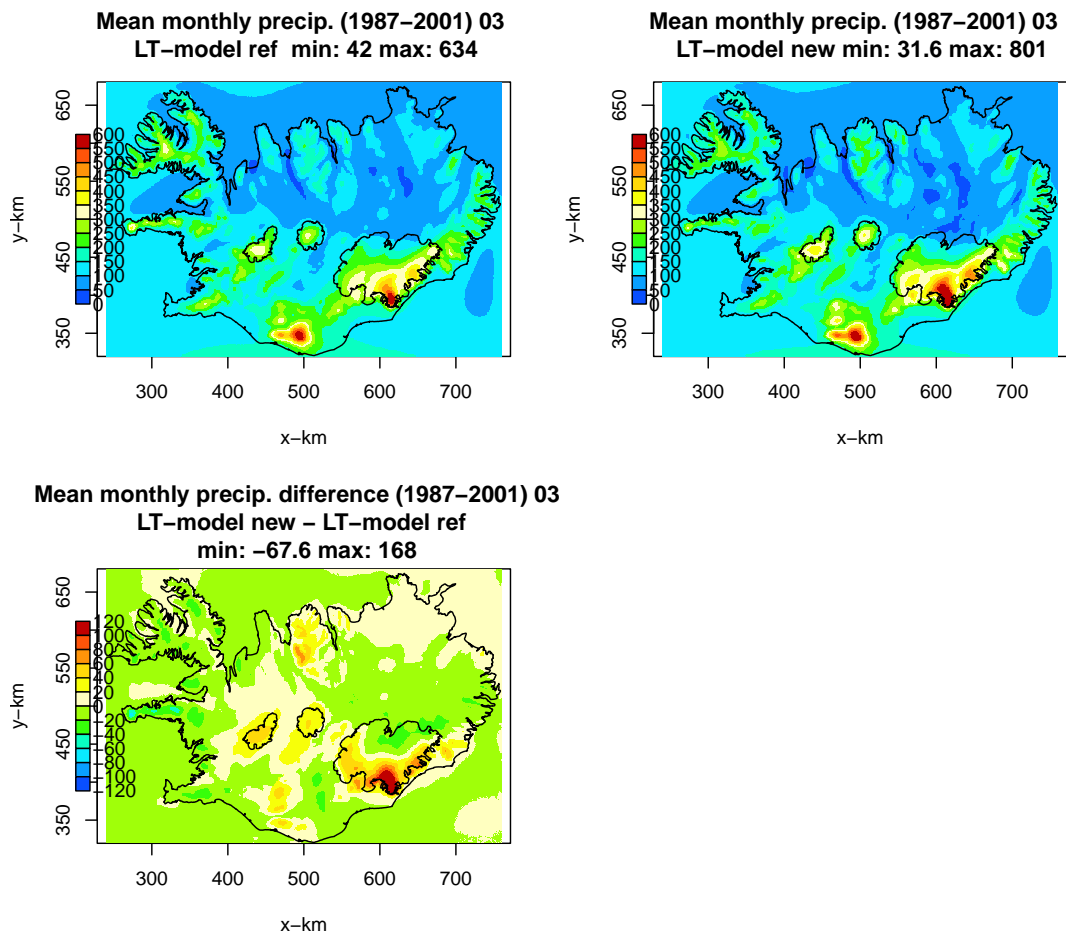


Figure VII.3. Mean March precipitation map (1987–2001) simulated with the reference model version (top-left) and the new model version (top-right), and the difference between the new and reference maps (bottom).

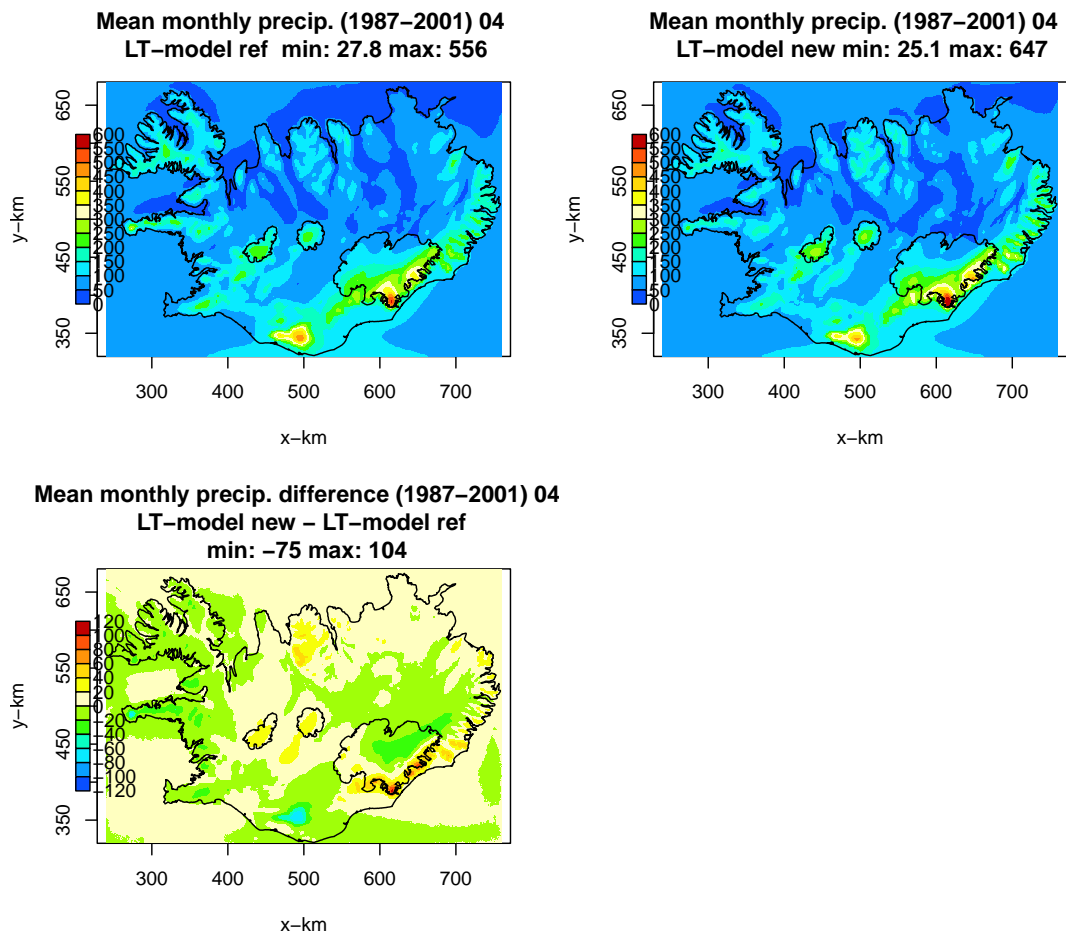


Figure VII.4. Mean April precipitation map (1987–2001) simulated with the reference model version (top-left) and the new model version (top-right), and the difference between the new and reference maps (bottom).

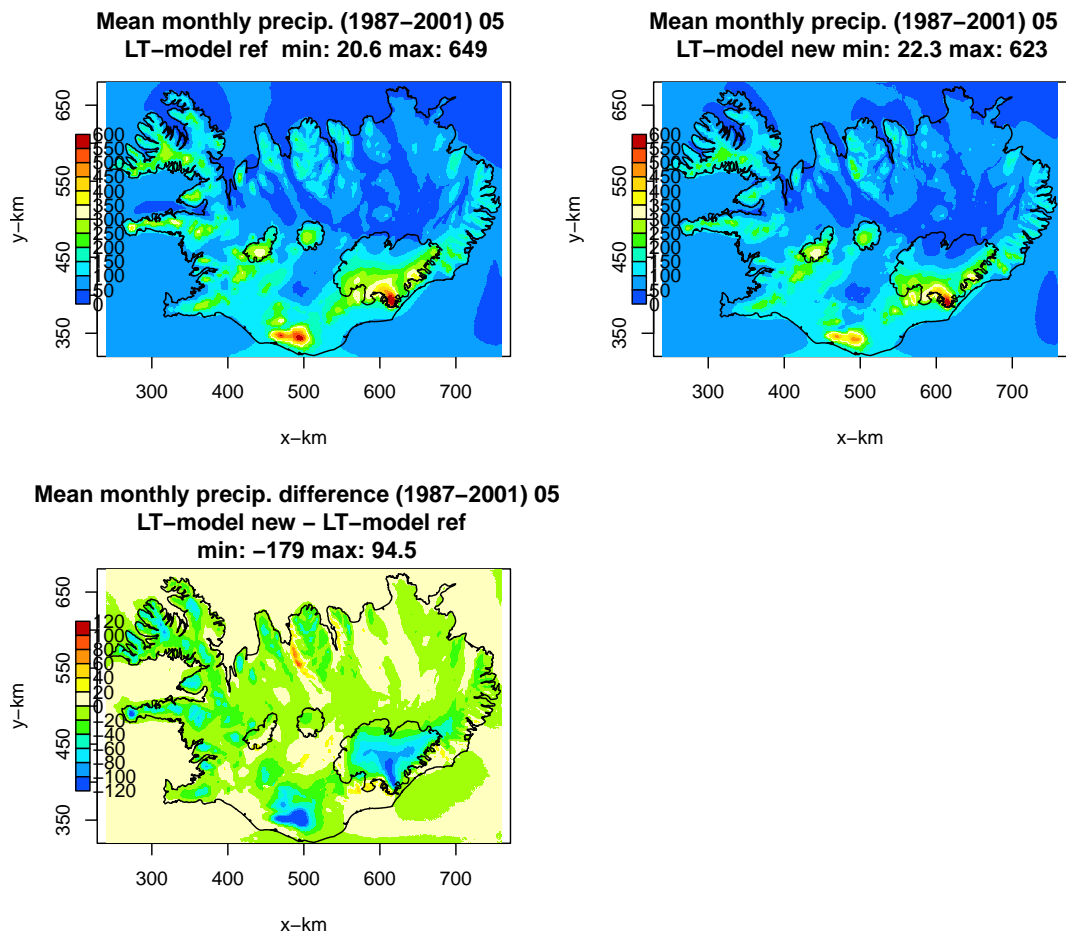


Figure VII.5. Mean May precipitation map (1987–2001) simulated with the reference model version (top-left) and the new model version (top-right), and the difference between the new and reference maps (bottom).

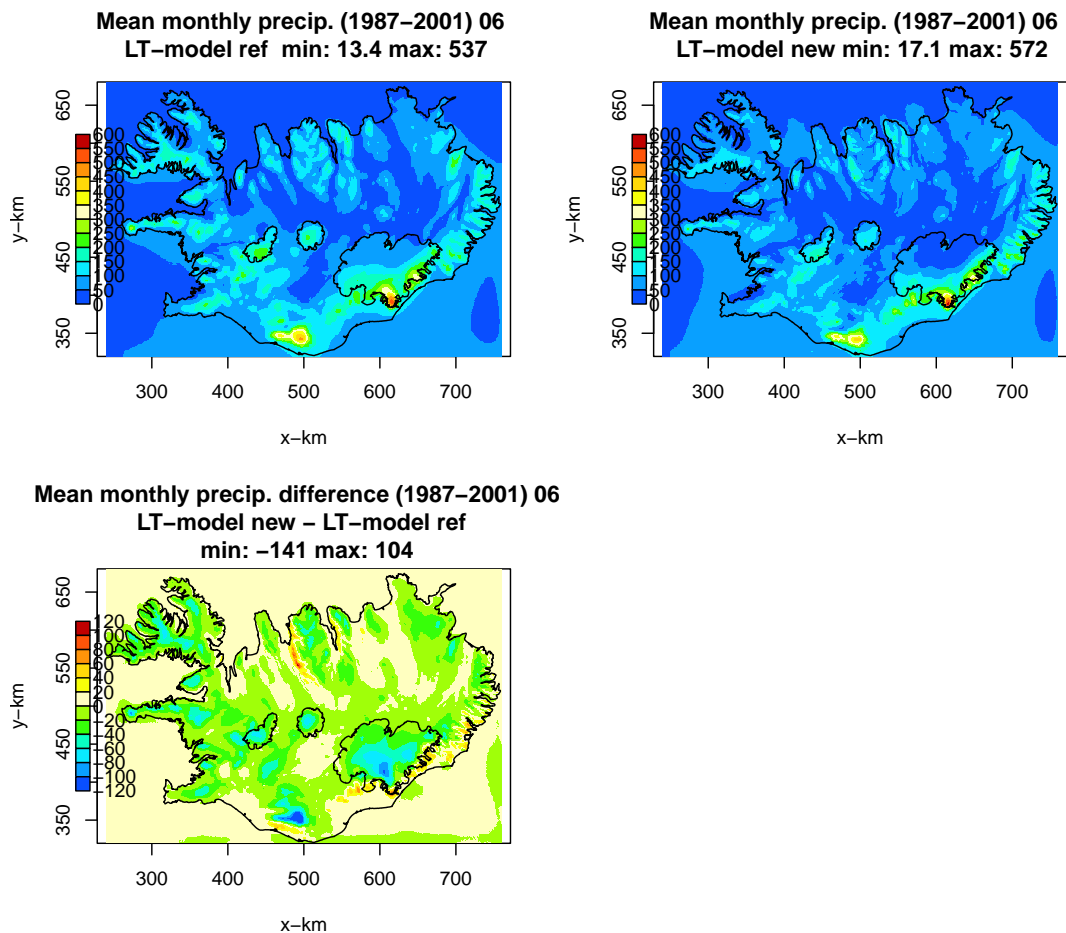


Figure VII.6. Mean June precipitation map (1987–2001) simulated with the reference model version (top-left) and the new model version (top-right), and the difference between the new and reference maps (bottom).

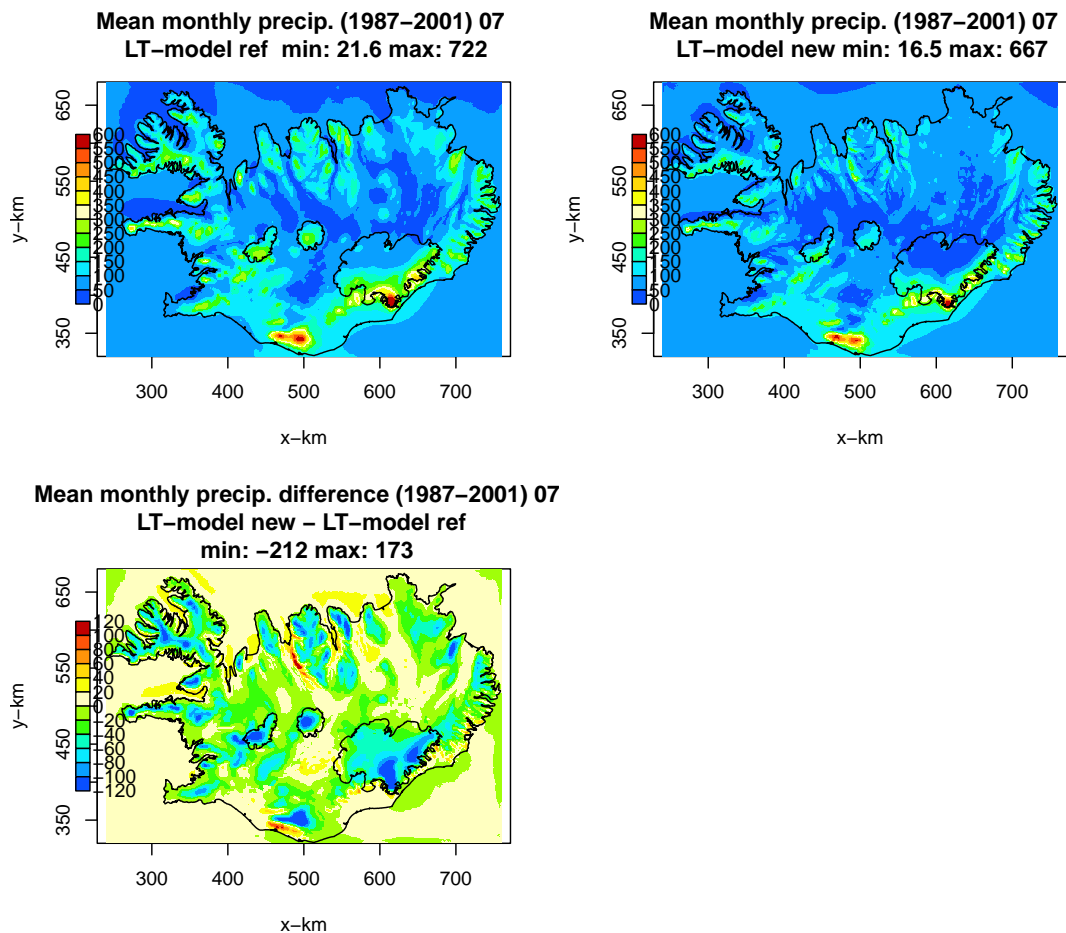


Figure VII.7. Mean July precipitation map (1987–2001) simulated with the reference model version (top-left) and the new model version (top-right), and the difference between the new and reference maps (bottom).

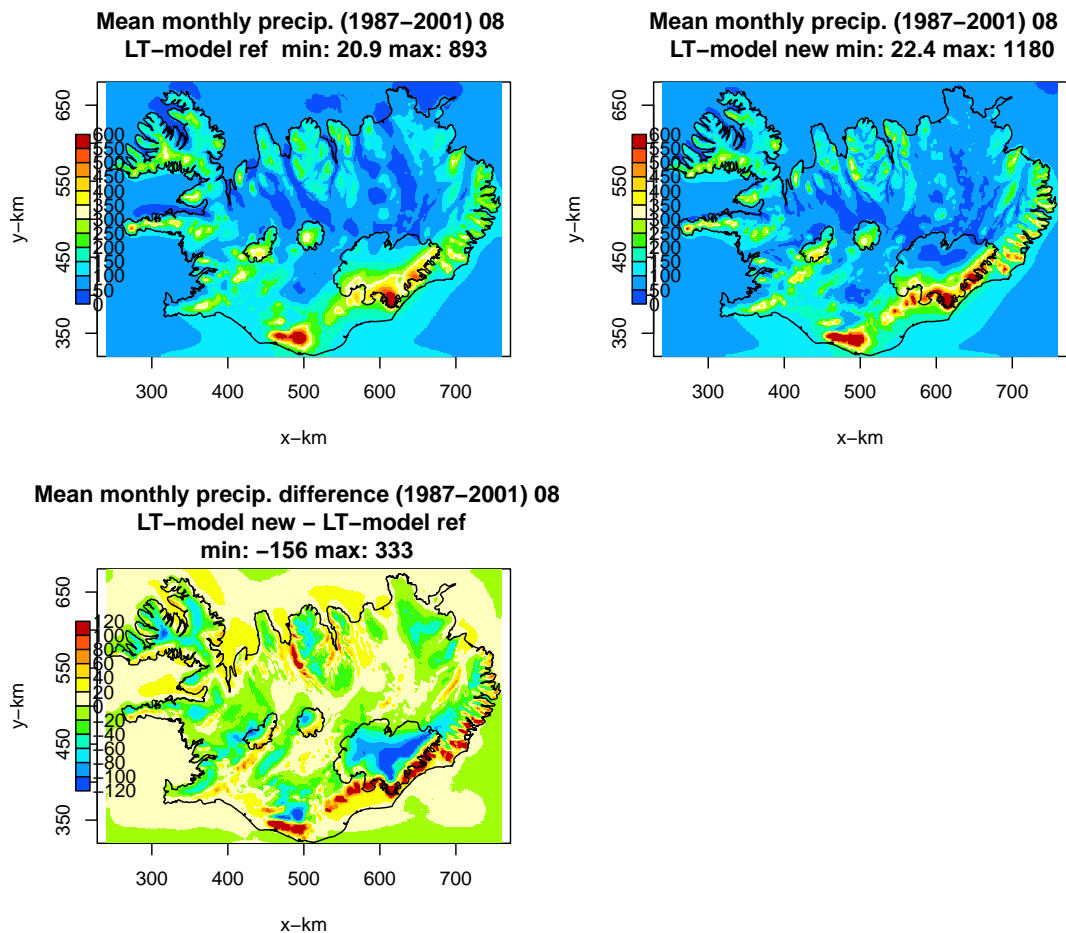


Figure VII.8. Mean August precipitation map (1987–2001) simulated with the reference model version (top-left) and the new model version (top-right), and the difference between the new and reference maps (bottom).

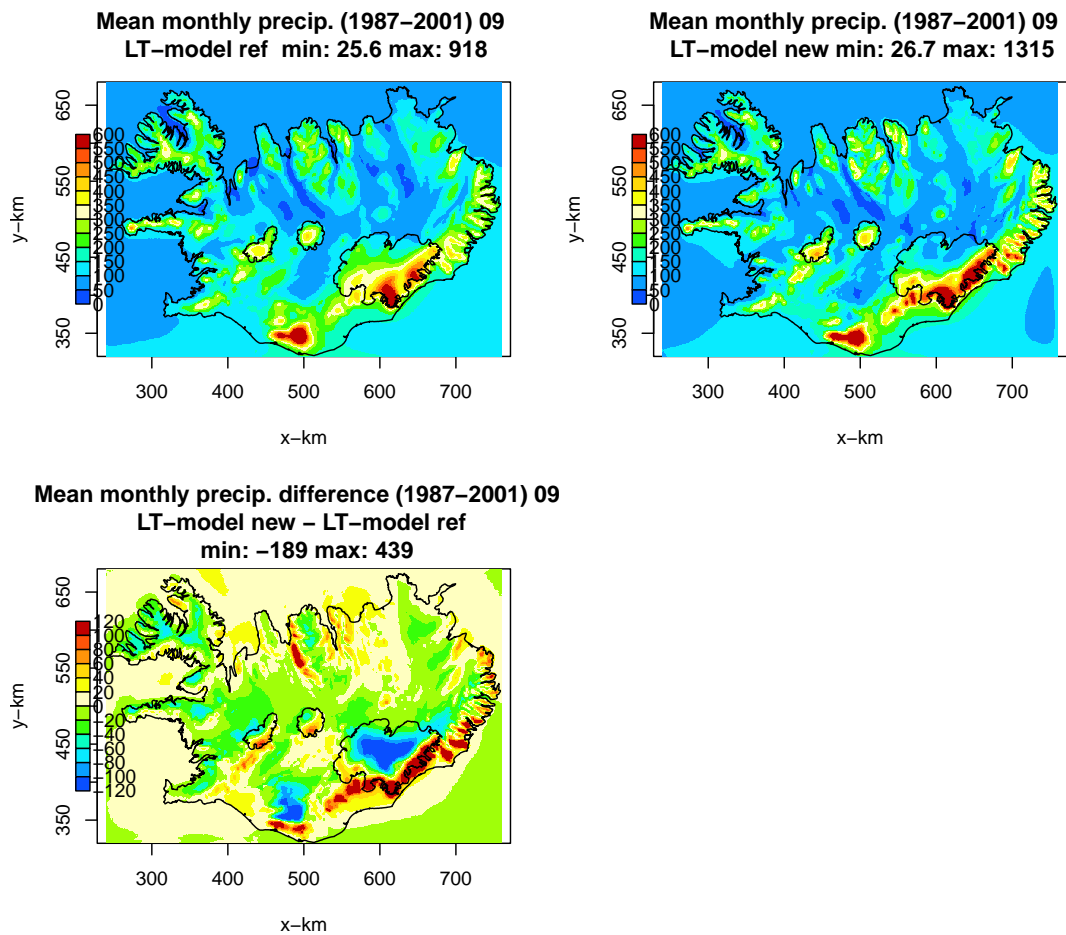


Figure VII.9. Mean September precipitation map (1987–2001) simulated with the reference model version (top-left) and the new model version (top-right), and the difference between the new and reference maps (bottom).

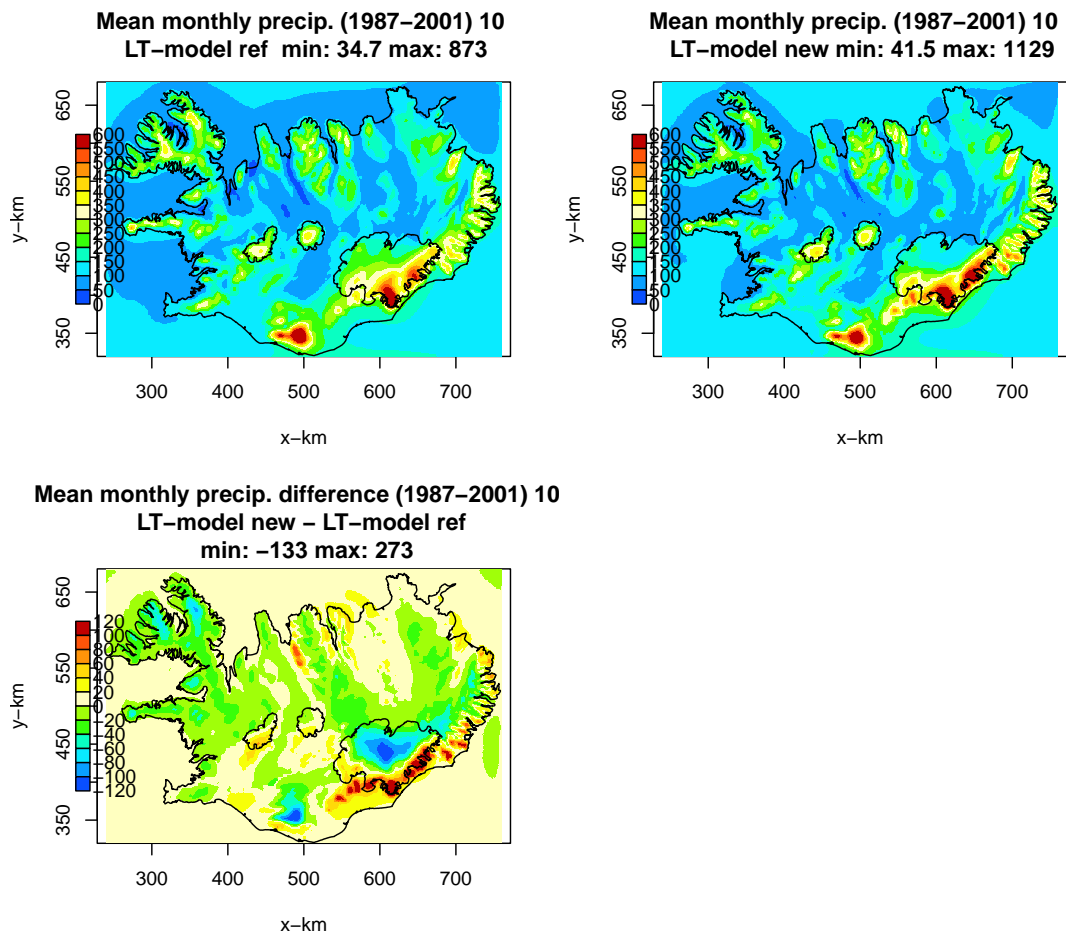


Figure VII.10. Mean October precipitation map (1987–2001) simulated with the reference model version (top-left) and the new model version (top-right), and the difference between the new and reference maps (bottom).

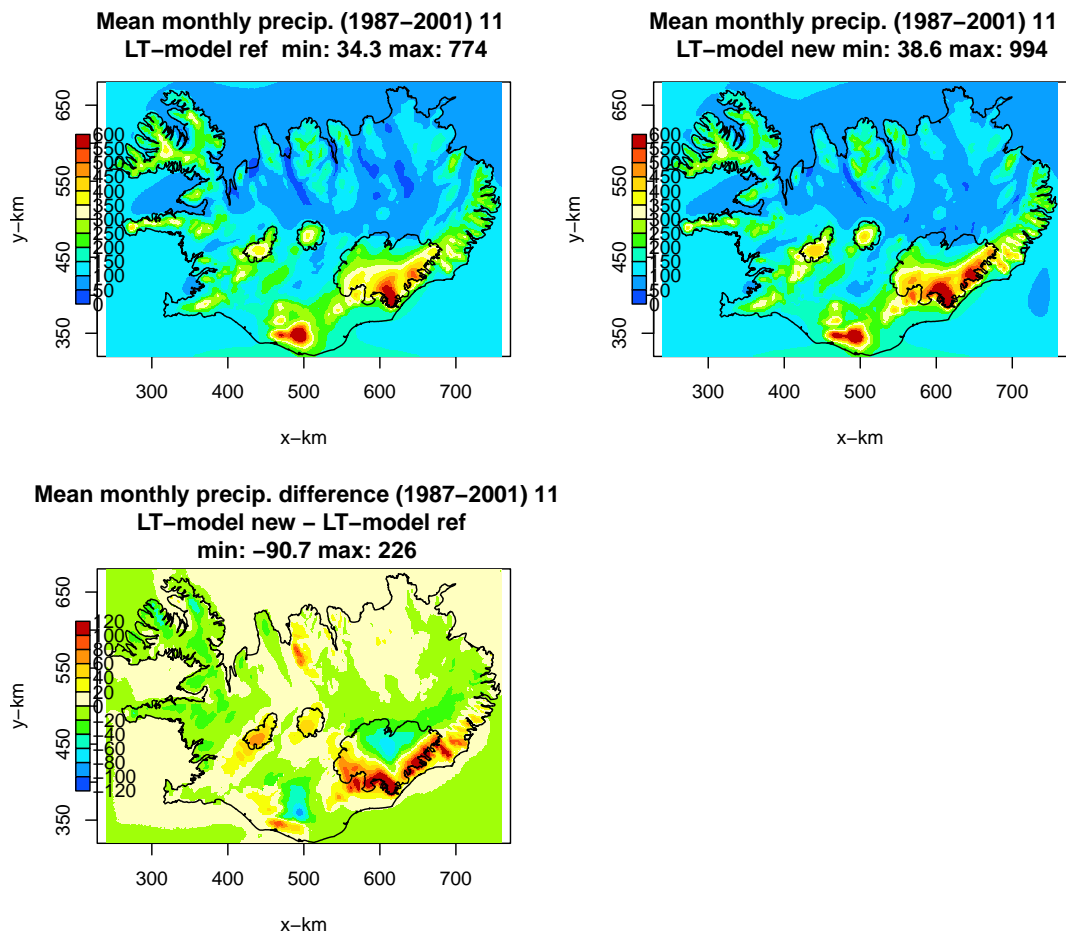


Figure VII.11. Mean November precipitation map (1987–2001) simulated with the reference model version (top-left) and the new model version (top-right), and the difference between the new and reference maps (bottom).

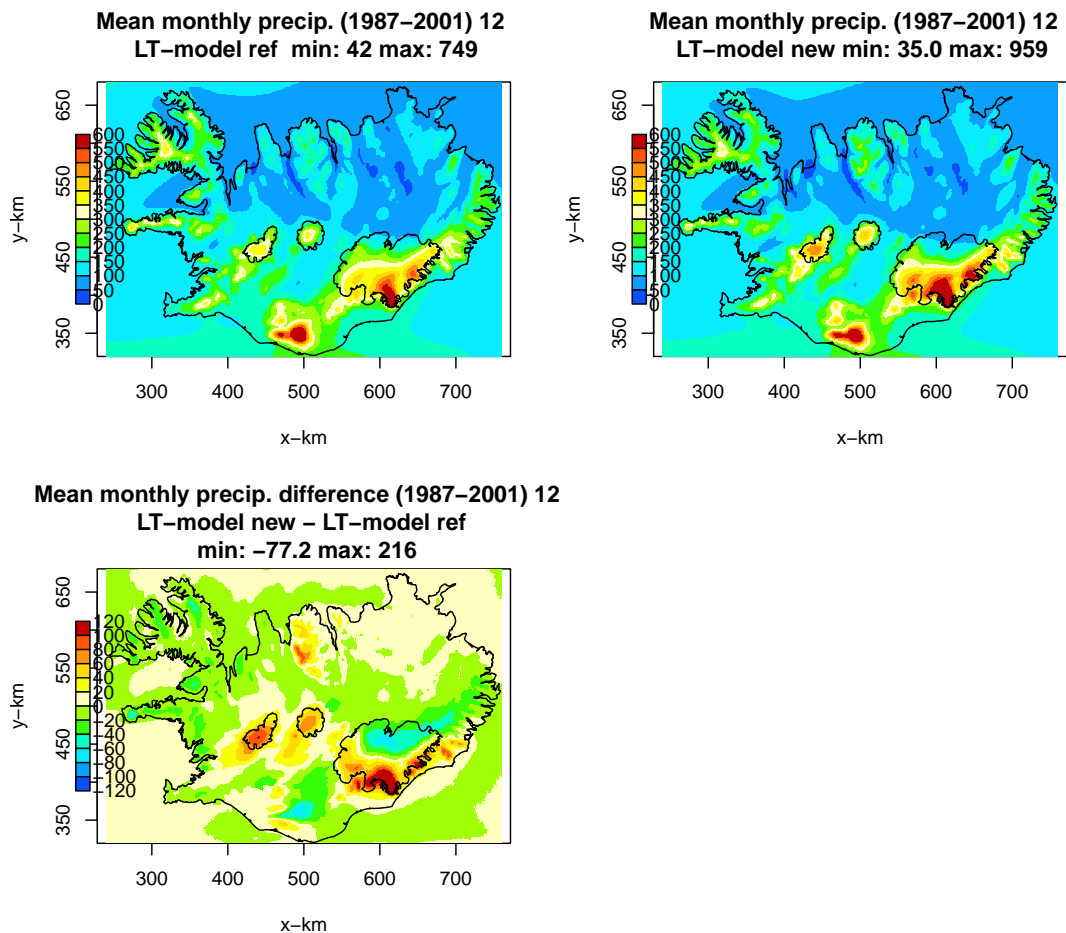


Figure VII.12. Mean December precipitation map (1987–2001) simulated with the reference model version (top-left) and the new model version (top-right), and the difference between the new and reference maps (bottom).